Supplementary Information (SI) for CrystEngComm.

Supporting Information

Three-Dimensional 14-Core Manganese-sodium based Polyoxometalate with unique Channels as bifunctional electrocatalysts for overall water splitting

Table of Contents

1 Experimental Procedures

1.1 Reagents and materials

All reagents were purchased from Shanghai Aladdin Biochemical Technology Co., Ltd., ≥ 99%(purity), on page 5-6 of the manuscript.

1.2 Electrode preparation

The carbon cloth was 1×1.5 cm^2 and was washed three times with 0.5 M H_2SO_4/deionized water and dried. The compound was fully ground into a powder and ground with acetylene black (Compound: Acetylene black =3:1). 5.0 mg mixture was fully mixed and dispersed in 200μL solution (ethanol: water =3:1) and sonicated for 30 minutes. The dispersed slurry (5μL) was dripped onto the carbon cloth electrode to form a uniform film at room temperature for 2 hours. Then the Nafion solution (5μL) was dripped on the electrode surface as a protective film and was dried for 1 hours.

1.3 Experimental procedure diagrams and tables

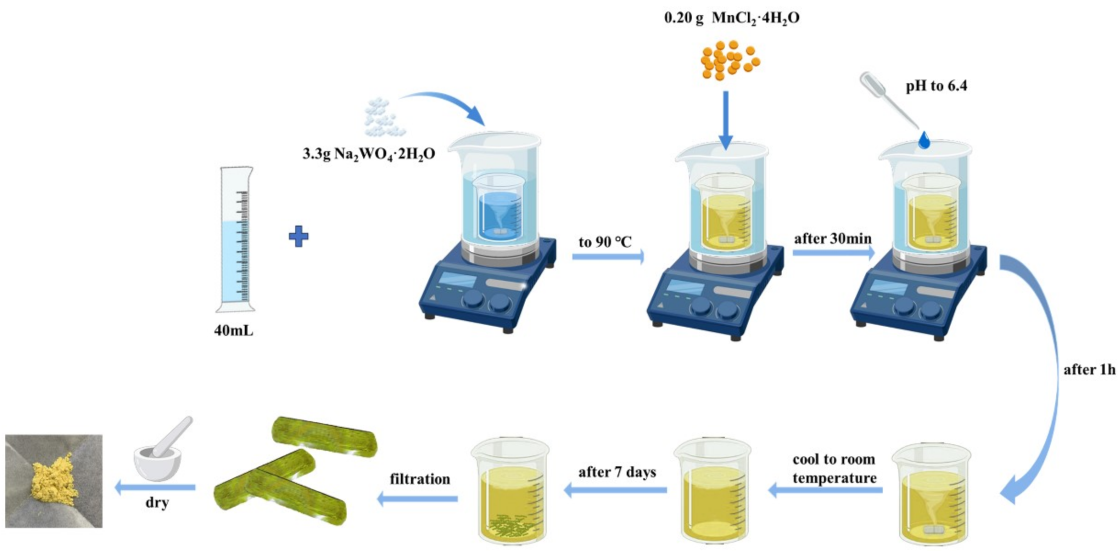

Figure S1 The synthetic process of Compound 1

Table S1 The synthetic conditions for Compounds 1-2

	$Na_2WO_4·2H_2O$	$MnCl_2·4H_2O$	$C_7H_{10}N_2$	pH	reaction temperature	Solution volume	crystal
1	10mmol	0.1mmol		6.4	90°C	40 mL	No
2	10mmol	0.5mmol		6.4	90°C	40 mL	No
3	10mmol	1mmol		6.4	90°C	40 mL	Compound 1
4	10mmol	2mmol		6.4	90°C	40 mL	No
5	10mmol	3mmol		6.4	90°C	40 mL	No
6	10mmol	1mmol		5.4	90°C	40 mL	No
7	10mmol	1mmol		5.8	90°C	40 mL	No
8	10mmol	1mmol		6.7	90°C	40 mL	No
9	10mmol	1mmol		6.4	80°C	40 mL	No
10	10mmol	1mmol		6.4	100°C	40 mL	No
11	10mmol	1mmol		6.4		20 mL	No
12	10mmol	1mmol		6.4		30 mL	No
13	10mmol	1mmol		6.4		50 mL	No
14	10mmol	1mmol		6.4		60 mL	No
15	10mmol		0.1mmol	6.7	90°C	40 mL	No
16	10mmol		0.5mmol	6.7	90°C	40 mL	No
17	10mmol		1mmol	6.7	90°C	40 mL	Compound 2
18	10mmol		2mmol	6.7	90°C	40 mL	No
19	10mmol		3mmol	6.7	90°C	40 mL	No
20	10mmol		1mmol	5.8	90°C	40 mL	No
21	10mmol		1mmol	6.4	90°C	40 mL	No
22	10mmol		1mmol	7.0	90°C	40 mL	No
23	10mmol		1mmol	6.7	80°C	40 mL	No
24	10mmol		1mmol	6.7	100°C	40 mL	No
25	10mmol		1mmol	6.7	90°C	20 mL	No
26	10mmol		1mmol	6.7	90°C	30 mL	No
27	10mmol		1mmol	6.7	90°C	50 mL	No
28	10mmol		1mmol	6.7	90°C	60 mL	No

1.4 Elemental percentage calculations

Table S2 The specific elemental analysis of Compounds 1-2

Compound	m(g)	V_0(mL)	element	C_0(mg/L)	C_x(mg/kg)	W(%)	At(%)	atoms ratio
Compound 1	0.1210	100	Na	89.56	74016.53	7.40%	3.22%	12.11
	0.1210	100	Mn	35.01	28933.88	2.89%	0.525%	1.97
	0.1210	100	W	721.11	595958.68	59.60%	3.24%	12.18
	0.1210	100	O	346.12	286049.59	28.60%	17.88%	67.22

Compound 2	0.1385	100	W	840.23	606664.26	60.67%	3.30%	12.00
	0.1385	100	O	261.24	188620.94	18.86%	11.79%	42.87
	0.1385	100	C	192.22	138787.00	13.88%	11.57%	42.07
	0.1385	100	N	63.56	45891.70	4.59%	3.28%	11.93

CN analysis was conducted using Thermo Scientific FLASH 2000 HT analyzer and ICP-OES analysis was performed using PerkinElmer optima 5300 DV ICP-OES.

$$C_x = \frac{C_0 * V_0}{m * 10^{-3}}$$

$$W(\%) = \frac{C_x}{10^6} * 100\%$$

$$A_t(\%) = \frac{W(\%)}{M}$$

m is the mass of the compound.
V_0 is the volume in a fixed volume
C_0 is the concentration of the element in the solution.
C_x is the unit mass of the elements in the compound.
W (%) is the weight percentage.
At (%) is the percentage of atoms.

2 Results and Discussion

2.1 Lengths and Angles Table

Table S3 Selected bond lengths (Å) and angles for Compound 1

W(1)-O(1)	**2.098(9)**	**W(1)-O(2)**	**2.261(9)**	**W(1)-O(8)**	**1.812(9)**
W(1)-O(10)	**1.719(9)**	**W(1)-O(12)**	**1.927(9)**	**W(1)-O(19)**	**1.926(9)**
W(2)-O(1)	**1.846(9)**	**W(2)-O(2)**	**2.238(9)**	**W(2)-O(6)**	**1.920(9)**
W(2)-O(11)	**1.970(10)**	**W(2)-O(15)**	**1.735(9)**	**W(2)-O(16)**	**1.874(10)**
W(3)-O(13)	**1.906(9)**	**W(3)-O(14)**	**2.304(10)**	**W(3)-O(17)**	**1.916(9)**
W(3)-O(18)	**1.751(9)**	**W(3)-O(19)**	**2.216(9)**	**W(3)-O(20)**	**1.739(11)**
W(4)-O(4)	**1.762(9)**	**W(4)-O(6)**	**1.893(9)**	**W(4)-O(7)**	**2.218(9)**
W(4)-O(9)	**1.745(11)**	**W(4)-O(17)**	**1.959(9)**	**W(4)-O(19)**	**2.187(9)**
W(5)-O(3)	**1.748(9)**	**W(5)-O(5)**	**1.731(9)**	**W(5)-O(8)**	**2.183(9)**
W(5)-O(11)	**1.847(10)**	**W(5)-O(13)**	**1.984(10)**	**W(5)-O(14)**	**2.220(9)**
W(6)-O(2)	**2.266(9)**	**W(6)-O(7)**	**1.803(9)**	**W(6)-O(12)**	**1.987(9)**
W(6)-O(14)	**1.888(9)**	**W(6)-O(16)**	**2.064(10)**	**W(6)-O(21)**	**1.721(9)**
O(1)-Na(4)	**2.969(15)**	**O(2)-W(6)**	**2.266(9)**	**O(3)-Mn(1)**	**2.426(9)**
O(3)-Na(6)	**2.463(11)**	**O(4)-Na(5)**	**2.916(14)**	**O(5)-Mn(1)**	**2.386(10)**
O(8)-W(5)	**2.183(9)**	**O(10)-Na(1)**	**2.415(10)**	**O(12)-W(6)**	**1.987(9)**

O(13)-W(5)	1.984(10)	O(14)-W(5)	2.220(9)	O(15)-Na(6)	2.393(10)
O(16)-W(6)	2.064(10)	O(20)-Na(3)	2.865(15)	O(21)-Mn(1)	2.447(9)
Mn(1)-O(3)	2.426(9)	Mn(1)-O(5)	2.386(10)	Mn(1)-O(22)	2.409(10)
Mn(1)-O(23)	2.398(10)	Mn(1)-O(24)	2.388(11)	Mn(1)-O(25)	2.381(11)
O(24)-Na(4)	2.818(16)	O(25)-Na(6)	2.347(12)	Na(1)-O(26)	2.347(11)
Na(1)-O(28)	2.389(12)	Na(1)-O(29)	2.389(12)	Na(1)-O(30)	2.515(12)
Na(1)-O(27)	2.352(12)	O(26)-Na(6)	2.389(10)	O(28)-Na(6)	2.337(12)
O(29)-Na(2)	2.448(12)	O(29)-Na(3)	2.814(15)	O(30)-Na(5)	2.762(15)
Na(2)-O(31)	2.377(12)	Na(2)-O(32)	2.457(12)	Na(2)-O(33)	2.612(12)
Na(2)-O(27)	2.328(12)	O(32)-Na(2)	2.457(12)	O(32)-Na(4)	2.806(16)
O(33)-Na(3)	2.789(16)	Na(4)-O(1)	2.969(15)	Na(4)-O(24)	2.818(16)
Na(4)-O(27)	2.850(16)	Na(5)-O(4)	2.916(14)	Na(6)-O(3)	2.463(11)
Na(6)-O(15)	2.393(10)	Na(6)-O(26)	2.389(10)	Na(6)-O(28)	2.337(12)
O(1)-W(1)-O(2)	72.0(4)	O(8)-W(1)-O(1)	161.1(4)	O(8)-W(1)-O(2)	89.1(4)
O(8)-W(1)-O(12)	92.5(4)	O(8)-W(1)-O(19)	94.0(4)	O(10)-W(1)-O(1)	95.6(4)
O(10)-W(1)-O(2)	165.4(4)	O(10)-W(1)-O(8)	103.3(4)	O(10)-W(1)-O(12)	99.8(4)
O(10)-W(1)-O(19)	101.3(4)	O(12)-W(1)-O(1)	82.4(4)	O(12)-W(1)-O(2)	71.6(3)
O(19)-W(1)-O(1)	84.0(4)	O(19)-W(1)-O(2)	85.3(4)	O(19)-W(1)-O(12)	155.9(4)
O(1)-W(2)-O(2)	77.2(4)	O(1)-W(2)-O(6)	88.4(4)	O(1)-W(2)-O(11)	156.6(4)
O(1)-W(2)-O(16)	90.7(4)	O(6)-W(2)-O(2)	80.7(4)	O(6)-W(2)-O(11)	85.0(4)
O(11)-W(2)-O(2)	79.6(4)	O(15)-W(2)-O(1)	104.0(4)	O(15)-W(2)-O(2)	177.9(4)
O(15)-W(2)-O(6)	101.0(4)	O(15)-W(2)-O(11)	99.3(4)	O(15)-W(2)-O(16)	102.5(4)
O(16)-W(2)-O(2)	75.7(4)	O(16)-W(2)-O(6)	155.9(4)	O(16)-W(2)-O(11)	86.3(4)
O(13)-W(3)-O(14)	73.6(4)	O(13)-W(3)-O(17)	153.1(4)	O(13)-W(3)-O(19)	87.1(4)
O(17)-W(3)-O(14)	83.5(4)	O(17)-W(3)-O(19)	74.1(4)	O(18)-W(3)-O(13)	97.8(4)
O(18)-W(3)-O(14)	88.9(4)	O(18)-W(3)-O(17)	95.5(4)	O(18)-W(3)-O(19)	163.5(4)
O(19)-W(3)-O(14)	77.4(3)	O(20)-W(3)-O(13)	98.8(4)	O(20)-W(3)-O(14)	168.1(4)
O(20)-W(3)-O(17)	101.3(4)	O(20)-W(3)-O(18)	101.4(5)	O(20)-W(3)-O(19)	93.3(4)
O(4)-W(4)-O(6)	99.0(4)	O(4)-W(4)-O(7)	87.8(4)	O(4)-W(4)-O(17)	94.4(4)
O(4)-W(4)-O(19)	161.7(4)	O(6)-W(4)-O(7)	82.6(4)	O(6)-W(4)-O(17)	157.8(4)
O(6)-W(4)-O(19)	88.3(4)	O(9)-W(4)-O(4)	102.5(5)	O(9)-W(4)-O(6)	97.1(4)
O(9)-W(4)-O(7)	169.6(4)	O(9)-W(4)-O(17)	97.2(4)	O(9)-W(4)-O(19)	93.2(4)
O(17)-W(4)-O(7)	80.3(4)	O(17)-W(4)-O(19)	74.0(4)	O(19)-W(4)-O(7)	76.4(3)
O(3)-W(5)-O(8)	90.9(4)	O(3)-W(5)-O(11)	100.1(4)	O(3)-W(5)-O(13)	94.4(4)
O(3)-W(5)-O(14)	164.3(4)	O(5)-W(5)-O(3)	103.0(4)	O(5)-W(5)-O(8)	164.7(4)
O(5)-W(5)-O(11)	99.6(4)	O(5)-W(5)-O(13)	94.5(4)	O(5)-W(5)-O(14)	88.8(4)
O(8)-W(5)-O(14)	76.5(3)	O(11)-W(5)-O(8)	84.2(4)	O(11)-W(5)-O(13)	156.9(4)
O(11)-W(5)-O(14)	87.9(4)	O(13)-W(5)-O(8)	77.6(4)	O(13)-W(5)-O(14)	74.1(4)
O(7)-W(6)-O(2)	88.7(4)	O(7)-W(6)-O(12)	92.0(4)	O(7)-W(6)-O(14)	95.5(4)
O(7)-W(6)-O(16)	160.3(4)	O(12)-W(6)-O(2)	70.5(3)	O(12)-W(6)-O(16)	80.8(4)
O(14)-W(6)-O(2)	88.1(4)	O(14)-W(6)-O(12)	157.2(4)	O(14)-W(6)-O(16)	85.1(4)
O(16)-W(6)-O(2)	71.6(3)	O(21)-W(6)-O(2)	162.5(4)	O(21)-W(6)-O(7)	103.1(4)
O(21)-W(6)-O(12)	95.9(4)	O(21)-W(6)-O(14)	103.4(4)	O(21)-W(6)-O(16)	95.9(4)
O(3)-Mn(1)-O(21)	125.8(3)	O(3)-Mn(1)-Na(6)	43.7(2)	O(5)-Mn(1)-O(3)	75.8(3)
O(5)-Mn(1)-O(21)	156.4(3)	O(5)-Mn(1)-O(22)	82.2(3)	O(5)-Mn(1)-O(23)	131.6(3)
O(5)-Mn(1)-O(24)	84.8(4)	O(22)-Mn(1)-O(3)	148.1(3)	O(22)-Mn(1)-O(21)	74.2(3)
O(23)-Mn(1)-O(3)	74.2(3)	O(23)-Mn(1)-O(21)	69.3(3)	O(23)-Mn(1)-O(22)	137.2(3)
O(24)-Mn(1)-O(3)	120.5(4)	O(24)-Mn(1)-O(21)	90.1(3)	O(24)-Mn(1)-O(22)	79.5(4)
O(24)-Mn(1)-O(23)	78.9(4)	O(25)-Mn(1)-O(3)	81.1(3)	O(25)-Mn(1)-O(5)	91.1(3)

O(25)-Mn(1)-O(21)	**84.2(3)**	**O(25)-Mn(1)-O(22)**	**76.5(4)**	**O(25)-Mn(1)-O(23)**	**120.2(4)**
O(25)-Mn(1)-O(24)	**155.9(4)**	**O(10)-Na(1)-O(30)**	**170.7(4)**	**O(10)-Na(1)-Na(2)**	**93.3(3)**
O(10)-Na(1)-Na(3)	**64.5(3)**	**O(10)-Na(1)-Na(5)**	**132.8(3)**	**O(26)-Na(1)-O(10)**	**89.3(4)**
O(26)-Na(1)-O(28)	**85.2(4)**	**O(26)-Na(1)-O(29)**	**162.0(4)**	**O(26)-Na(1)-O(30)**	**82.9(4)**
O(26)-Na(1)-O(27)	**98.4(4)**	**O(28)-Na(1)-O(10)**	**80.2(4)**	**O(28)-Na(1)-O(29)**	**94.2(4)**
O(28)-Na(1)-O(30)	**103.9(4)**	**O(29)-Na(1)-O(10)**	**108.4(4)**	**O(29)-Na(1)-O(30)**	**79.8(4)**
O(27)-Na(1)-O(10)	**78.7(4)**	**O(27)-Na(1)-O(28)**	**158.6(4)**	**O(27)-Na(1)-O(29)**	**88.8(4)**
O(27)-Na(1)-O(30)	**97.5(4)**	**O(29)-Na(2)-O(32)**	**103.0(4)**	**O(29)-Na(2)-O(32)**	**163.9(5)**
O(29)-Na(2)-O(33)	**80.0(4)**	**O(31)-Na(2)-O(29)**	**82.8(4)**	**O(31)-Na(2)-O(32)**	**103.7(4)**
O(31)-Na(2)-O(33)	**88.7(4)**	**O(32)-Na(2)-O(32)**	**88.6(4)**	**O(32)-Na(2)-O(33)**	**160.5(5)**
O(27)-Na(2)-O(29)	**87.9(4)**	**O(27)-Na(2)-O(31)**	**168.4(5)**	**O(27)-Na(2)-O(32)**	**78.2(4)**
O(27)-Na(2)-O(32)	**83.5(4)**	**O(27)-Na(2)-O(33)**	**82.8(4)**	**O(29)-Na(3)-O(20)**	**140.3(5)**
O(33)-Na(3)-O(20)	**118.1(5)**	**O(33)-Na(3)-O(29)**	**71.1(4)**	**O(24)-Na(4)-O(1)**	**137.6(5)**
O(24)-Na(4)-O(27)	**91.5(4)**	**O(32)-Na(4)-O(1)**	**123.7(5)**	**O(32)-Na(4)-O(24)**	**98.3(5)**
O(32)-Na(4)-O(27)	**68.6(4)**	**O(27)-Na(4)-O(1)**	**97.9(5)**	**O(30)-Na(5)-O(4)**	**98.9(4)**
O(15)-Na(6)-O(3)	**97.5(4)**	**O(25)-Na(6)-O(3)**	**81.0(4)**	**O(25)-Na(6)-O(15)**	**90.6(4)**
O(25)-Na(6)-O(26)	**83.1(4)**	**O(26)-Na(6)-O(3)**	**81.7(4)**	**O(26)-Na(6)-O(15)**	**173.6(4)**
O(28)-Na(6)-O(3)	**96.5(4)**	**O(28)-Na(6)-O(15)**	**101.0(4)**	**O(28)-Na(6)-O(25)**	**168.4(4)**
O(28)-Na(6)-O(26)	**85.4(4)**				

```
Alert level B
PLAT097_ALERT_2_B Large Reported Max.  (Positive) Residual Density       7.85 eA-3
             W5      W6
PLAT355_ALERT_3_B Long   O-H (X0.82,N0.98A)  O23       - H23      .       1.09 Ang.
PLAT420_ALERT_2_B D-H Bond Without Acceptor  O29       --H29      .     Please Check
```

PLAT097_ALERT_2_B: Compound 1 was sealed in a glass tube by he single crystal X-ray diffraction. W5 and W6 in compound 1 have a low temperature factor, which may be due to the crystal quality. We tested the single crystal X-ray diffraction of the three synthetic single crystals of compound 1, and the results showed that W5 and W6 still have these problems.

PLAT355_ALERT_2_B and PLAT420_ALERT_2_B:These two alert are hydrogen bonding problems attributed to free water molecules and do not affect the main structure.

```
Alert level B
PLAT342_ALERT_3_B Low Bond Precision on  C-C Bonds ...............    0.02792 Ang.
PLAT412_ALERT_2_B Short Intra XH3 .. XHn      H8        ..H17C      .      1.79 Ang.
                                                       x,y,z  =      1_555 Check
PLAT420_ALERT_2_B D-H Bond Without Acceptor  O41       --H41D      .    Please Check
PLAT420_ALERT_2_B D-H Bond Without Acceptor  O41       --H41E      .    Please Check
PLAT420_ALERT_2_B D-H Bond Without Acceptor  O43       --H43B      .    Please Check
PLAT430_ALERT_2_B Short Inter D...A Contact  O22       ..N8        .      2.74 Ang.
                                                       x,y,z  =      1_555 Check
PLAT430_ALERT_2_B Short Inter D...A Contact  O24       ..N10       .      2.69 Ang.
                                                    1+x,y,z  =      1_655 Check
```

PLAT342_ALERT_3_B：Compound 2 was sealed in a glass tube by he single crystal X-ray diffraction. This test method may cause the problem of low bond precision on C-C bonds.We tested the single crystal X-ray diffraction of the three synthetic single crystals of compound 2, and the results showed that low bond precision on C-C bonds still exist.

PLAT412_ALERT_2_B, PLAT420_ALERT_2_B and PLAT430_ALERT_2_B:These two alert are hydrogen bonding problems attributed to free water molecules and do not affect the main structure.

Table S4 Selected bond lengths (Å) and angles for Compound 2

W(1)-O(7)	1.890(12)	W(1)-O(10)	1.937(13)	W(1)-O(15)	1.919(10)
W(1)-O(33)	1.930(11)	W(1)-O(36)	2.248(11)	W(1)-O(37)	1.710(12)
W(2)-W(11)	3.2330(10)	W(2)-O(2)	2.175(10)	W(2)-O(7)	1.948(12)
W(2)-O(19)	1.917(12)	W(2)-O(24)	1.948(10)	W(2)-O(27)	1.885(12)
W(2)-O(35)	1.735(12)	W(3)-O(1)	1.897(12)	W(3)-O(4)	1.899(10)
W(3)-O(8)	1.944(11)	W(3)-O(11)	2.218(11)	W(3)-O(39)	1.705(12)
W(3)-O(40)	1.918(12)	W(4)-O(3)	1.882(11)	W(4)-O(16)	1.892(11)
W(4)-O(31)	1.947(13)	W(4)-O(33)	1.957(11)	W(4)-O(34)	1.685(11)
W(4)-O(36)	2.283(11)	W(5)-W(8)	3.2324(10	W(5)-O(14)	1.938(12)
W(5)-O(15)	1.884(11)	W(5)-O(25)	1.919(12)	W(5)-O(26)	1.720(11)
W(5)-O(27)	1.935(12)	W(5)-O(29)	2.193(11)	W(6)-O(1)	1.951(11)
W(6)-O(11)	2.270(11)	W(6)-O(21)	1.923(10)	W(6)-O(22)	1.932(11)
W(6)-O(28)	1.732(12)	W(6)-O(32)	1.901(11)	W(7)-O(2)	2.158(10)
W(7)-O(9)	1.711(10)	W(7)-O(12)	1.962(10)	W(7)-O(18)	1.922(11)
W(7)-O(24)	1.951(11)	W(7)-O(31)	1.886(12)	W(8)-O(5)	1.914(11)
W(8)-O(6)	1.921(11)	W(8)-O(21)	1.891(10)	W(8)-O(23)	1.735(12)
W(8)-O(25)	1.951(11)	W(8)-O(29)	2.198(12)	W(9)-O(4)	1.922(11)
W(9)-O(5)	1.924(11)	W(9)-O(13)	1.698(12)	W(9)-O(14)	1.943(11)
W(9)-O(17)	1.904(11)	W(9)-O(29)	2.196(11)	W(10)-O(8)	1.919(11)
W(10)-O(11)	2.217(11)	W(10)-O(16)	1.920(11)	W(10)-O(18)	1.888(11)
W(10)-O(22)	1.954(12)	W(10)-O(30)	1.731(11)	W(11)-O(2)	2.171(11)
W(11)-O(12)	1.920(10)	W(11)-O(17)	1.931(11)	W(11)-O(19)	1.962(11)
W(11)-O(38)	1.740(12)	W(11)-O(40)	1.906(11)	W(12)-O(3)	1.972(11)
W(12)-O(6)	1.894(11)	W(12)-O(10)	1.924(11)	W(12)-O(20)	1.726(13)
W(12)-O(32)	1.949(11)	W(12)-O(36)	2.217(12)		
O(7)-W(1)-O(10)	161.7(5)	O(7)-W(1)-O(15)	85.4(5)	O(7)-W(1)-O(33)	91.6(5)
O(7)-W(1)-O(36)	88.4(4)	O(10)-W(1)-O(36)	74.0(4)	O(15)-W(1)-O(10)	88.2(5)
O(15)-W(1)-O(33)	160.2(5)	O(15)-W(1)-O(36)	85.1(4)	O(33)-W(1)-O(10)	88.6(5)
O(33)-W(1)-O(36)	75.2(4)	O(37)-W(1)-O(7)	101.5(5)	O(37)-W(1)-O(10)	96.6(5)
O(37)-W(1)-O(15)	102.6(5)	O(37)-W(1)-O(33)	97.2(5)	O(37)-W(1)-O(36)	167.9(5)
O(2)-W(2)-W(11)	41.9(3)	O(7)-W(2)-W(11)	130.2(3)	O(7)-W(2)-O(2)	88.4(4)
O(7)-W(2)-O(24)	87.1(4)	O(19)-W(2)-W(11)	34.0(3)	O(19)-W(2)-O(2)	75.9(4)
O(19)-W(2)-O(7)	164.2(5)	O(19)-W(2)-O(24)	90.6(4)	O(24)-W(2)-O(2)	74.9(4)
O(27)-W(2)-O(2)	90.1(5)	O(27)-W(2)-O(7)	84.0(5)	O(27)-W(2)-O(19)	94.0(5)
O(27)-W(2)-O(24)	162.8(5)	O(35)-W(2)-O(2)	166.6(5)	O(35)-W(2)-O(7)	99.9(5)
O(35)-W(2)-O(19)	95.9(5)	O(35)-W(2)-O(24)	94.9(5)	O(35)-W(2)-O(27)	101.1(5)
O(1)-W(3)-O(4)	89.9(5)	O(1)-W(3)-O(8)	88.5(5)	O(1)-W(3)-O(11)	74.0(4)
O(1)-W(3)-O(40)	159.0(5)	O(4)-W(3)-O(8)	160.0(5)	O(4)-W(3)-O(11)	86.8(4)
O(4)-W(3)-O(40)	85.7(5)	O(8)-W(3)-O(11)	73.6(4)	O(39)-W(3)-O(1)	99.5(6)
O(39)-W(3)-O(4)	102.8(5)	O(39)-W(3)-O(8)	97.1(5)	O(39)-W(3)-O(11)	168.5(5)
O(39)-W(3)-O(40)	101.6(6)	O(40)-W(3)-O(8)	88.7(5)	O(40)-W(3)-O(11)	85.2(5)
O(3)-W(4)-O(16)	92.5(5)	O(3)-W(4)-O(31)	160.0(4)	O(3)-W(4)-O(33)	89.9(5)
O(3)-W(4)-O(36)	74.8(4)	O(16)-W(4)-O(31)	84.2(5)	O(16)-W(4)-O(33)	159.3(5)
O(16)-W(4)-O(36)	86.9(4)	O(31)-W(4)-O(33)	86.6(5)	O(31)-W(4)-O(36)	85.3(4)
O(34)-W(4)-O(3)	100.4(5)	O(33)-W(4)-O(36)	73.9(4)	O(34)-W(4)-O(16)	103.4(5)
O(34)-W(4)-O(31)	99.6(5)	O(34)-W(4)-O(33)	96.3(5)	O(34)-W(4)-O(36)	168.9(5)
O(14)-W(5)-O(29)	74.0(4)	O(15)-W(5)-O(14)	161.8(5)	O(15)-W(5)-O(25)	92.7(5)
O(15)-W(5)-O(27)	83.4(5)	O(15)-W(5)-O(29)	89.2(4)	O(25)-W(5)-O(14)	90.2(5)
O(25)-W(5)-O(27)	163.9(5)	O(25)-W(5)-O(29)	76.3(4)	O(26)-W(5)-O(14)	96.3(5)

O(26)-W(5)-O(15)	101.2(5)	O(26)-W(5)-O(25)	96.7(5)	O(26)-W(5)-O(27)	99.4(5)
O(26)-W(5)-O(29)	167.8(5)	O(27)-W(5)-O(14)	88.8(5)	O(27)-W(5)-O(29)	88.0(5)
O(1)-W(6)-O(11)	71.8(4)	O(21)-W(6)-O(1)	88.6(5)	O(21)-W(6)-O(11)	87.6(5)
O(21)-W(6)-O(22)	160.8(5)	O(22)-W(6)-O(1)	87.6(5)	O(22)-W(6)-O(11)	73.3(4)
O(28)-W(6)-O(10	97.5(6)	O(28)-W(6)-O(11)	165.7(5)	O(28)-W(6)-O(21)	102.0(5)
O(28)-W(6)-O(22)	97.1(5)	O(28)-W(6)-O(32)	101.4(6)	O(32)-W(6)-O(1)	161.1(5)
O(32)-W(6)-O(11)	89.5(5)	O(32)-W(6)-O(21)	87.6(5)	O(32)-W(6)-O(22)	89.9(5)
O(9)-W(7)-O(2)	164.2(5)	O(9)-W(7)-O(12)	94.5(5)	O(9)-W(7)-O(18)	102.6(5)
O(9)-W(7)-O(24)	93.1(5)	O(9)-W(7)-O(31)	100.7(5)	O(12)-W(7)-O(2)	75.2(4)
O(18)-W(7)-O(2)	89.0(4)	O(18)-W(7)-O(12)	87.1(5)	O(18)-W(7)-O(24)	164.2(4)
O(24)-W(7)-O(2)	75.3(4)	O(24)-W(7)-O(12)	90.2(5)	O(31)-W(7)-O(2)	90.6(4)
O(31)-W(7)-O(12)	164.6(4)	O(31)-W(7)-O(18)	86.7(5)	O(31)-W(7)-O(24)	91.9(5)
O(5)-W(8)-O(6)	160.1(5)	O(5)-W(8)-O(25)	91.5(5)	O(5)-W(8)-O(29)	74.3(4)
O(6)-W(8)-O(25)	87.2(5)	O(6)-W(8)-O(29)	86.2(4)	O(21)-W(8)-O(5)	89.9(5)
O(21)-W(8)-O(6)	85.5(5)	O(21)-W(8)-O(25)	162.4(5)	O(21)-W(8)-O(29)	87.9(5)
O(23)-W(8)-O(5)	100.0(5)	O(23)-W(8)-O(6)	99.8(5)	O(23)-W(8)-O(21)	100.4(5)
O(23)-W(8)-O(25)	96.7(5)	O(23)-W(8)-O(29)	170.1(5)	O(25)-W(8)-O(29)	75.6(4)
O(4)-W(9)-O(5)	88.2(5)	O(4)-W(9)-O(14)	161.4(5)	O(4)-W(9)-O(29)	87.7(5)
O(5)-W(9)-O(14)	89.0(5)	O(5)-W(9)-O(29)	74.2(4)	O(13)-W(9)-O(4)	102.2(5)
O(13)-W(9)-O(5)	97.5(6)	O(13)-W(9)-O(14)	96.4(5)	O(13)-W(9)-O(17)	100.6(6)
O(13)-W(9)-O(29)	167.0(5)	O(14)-W(9)-O(29)	73.8(4)	O(17)-W(9)-O(4)	86.2(5)
O(17)-W(9)-O(5)	161.8(5)	O(17)-W(9)-O(14)	90.8(5)	O(17)-W(9)-O(29)	88.3(5)
O(8)-W(10)-O(11)	74.1(4)	O(8)-W(10)-O(16)	160.8(5)	O(8)-W(10)-O(22)	89.1(5)
O(16)-W(10)-O(11)	86.7(4)	O(16)-W(10)-O(22)	87.4(5)	O(18)-W(10)-O(8)	91.2(5)
O(18)-W(10)-O(11)	86.6(4)	O(18)-W(10)-O(16)	85.8(5)	O(18)-W(10)-O(22)	159.9(5)
O(22)-W(10)-O(11)	74.2(4)	O(30)-W(10)-O(8)	96.8(5)	O(30)-W(10)-O(11)	167.5(5)
O(30)-W(10)-O(16)	102.4(5)	O(30)-W(10)-O(18)	102.5(5)	O(30)-W(10)-O(22)	97.4(5)
O(12)-W(11)-O(2)	75.7(4) .	O(12)-W(11)-O(17)	162.3(5)	O(12)-W(11)-O(19)	91.2(5)
O(17)-W(11)-O(2)	87.0(4)	O(17)-W(11)-O(19)	87.6(4)	O(19)-W(11)-O(2)	75.1(5)
O(38)-W(11)-O(2)	169.5(5)	O(38)-W(11)-O(12)	98.5(5)	O(38)-W(11)-O(17)	99.2(5)
O(38)-W(11)-O(19)	96.6(6)	O(38)-W(11)-O(40)	99.5(6)	O(40)-W(11)-O(2)	89.4(5)
O(40)-W(11)-O(12)	91.1(5)	O(40)-W(11)-O(17)	85.2(5)	O(40)-W(11)-O(19)	163.2(5)
O(3)-W(12)-O(36)	74.8(4)	O(6)-W(12)-O(3)	160.1(5)	O(6)-W(12)-O(10)	92.3(4)
O(6)-W(12)-O(32)	86.3(4)	O(6)-W(12)-O(36)	86.5(4)	O(10)-W(12)-O(3)	89.3(5)
O(10)-W(12)-O(32)	161.6(5)	O(10)-W(12)-O(36)	75.0(5)	O(20)-W(12)-O(3)	97.8(5)
O(20)-W(12)-O(6)	101.5(5)	O(20)-W(12)-O(10)	100.2(6)	O(20)-W(12)-O(32)	98.1(6)
O(20)-W(12)-O(36)	171.0(5)	O(32)-W(12)-O(3)	85.9(5)	O(32)-W(12)-O(36)	86.6(5)

2.2 The structural diagrams of compounds 1-2

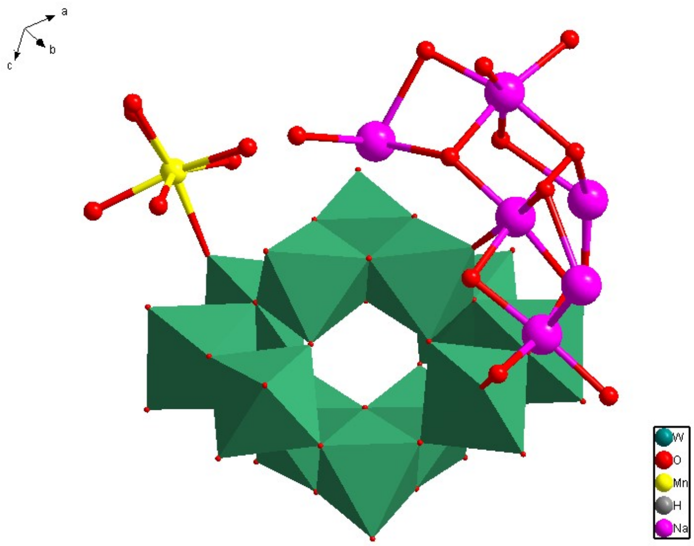

Figure S2 monomer diagram of Compound 1

(a)

(b)

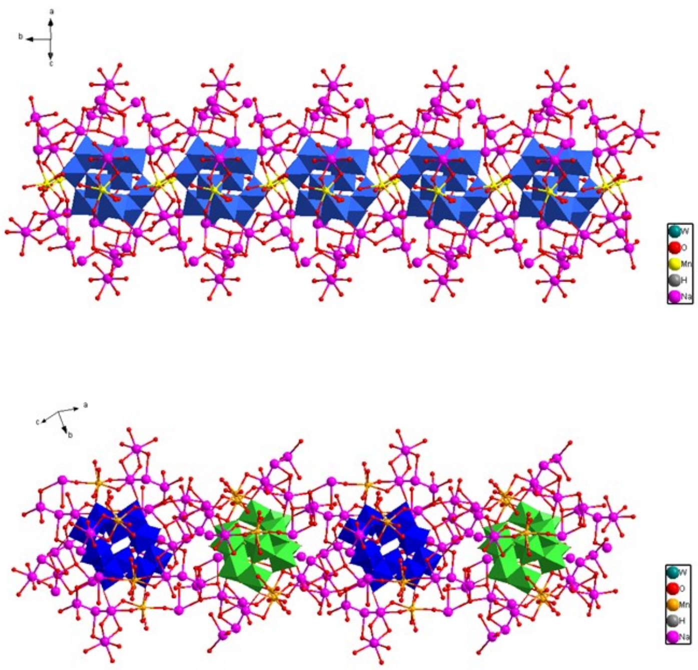

Figure S3 (a) Views of 1D-1 chain structure of Compound 1 (b) Views of 1D-2 chain of Compound 1

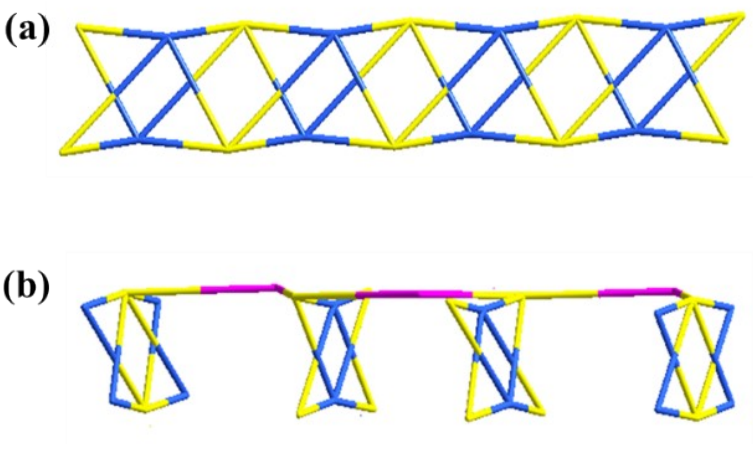

Figure S4 (a) The simplified diagram of 1D-1 (b) The simplified diagram of 1D-2

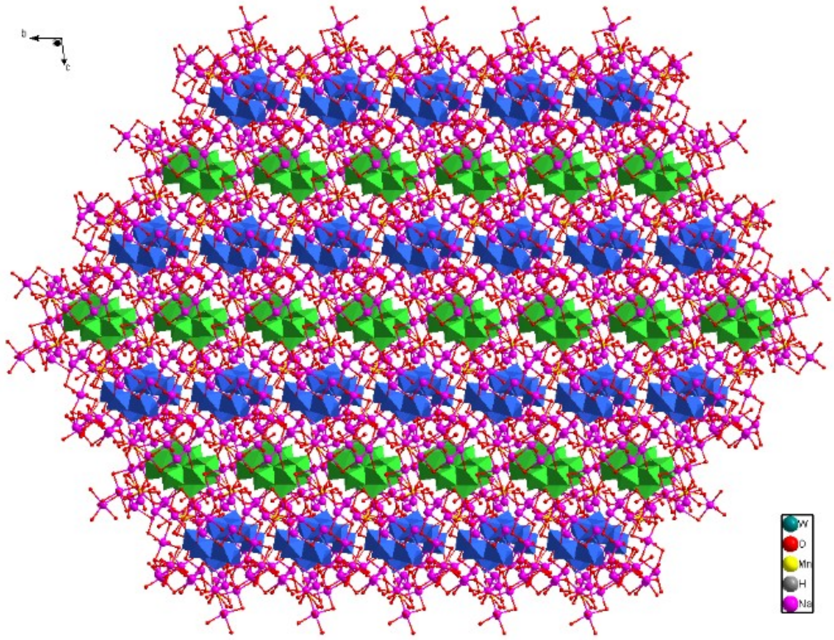

Figure S5 Views of 2D-1 structure of layer structure of Compound 1

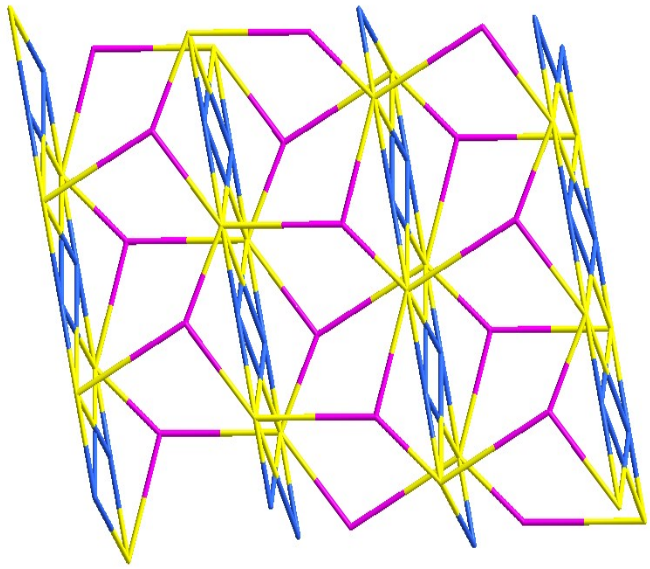

Figure S6 The simplified diagram of 2D-1

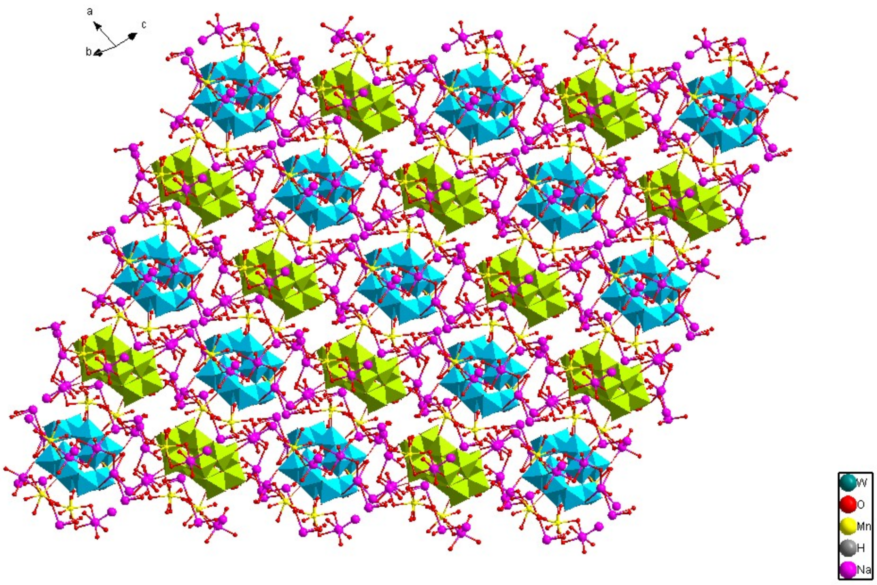

Figure S7 Views of 2D-2 structure of Compound 1

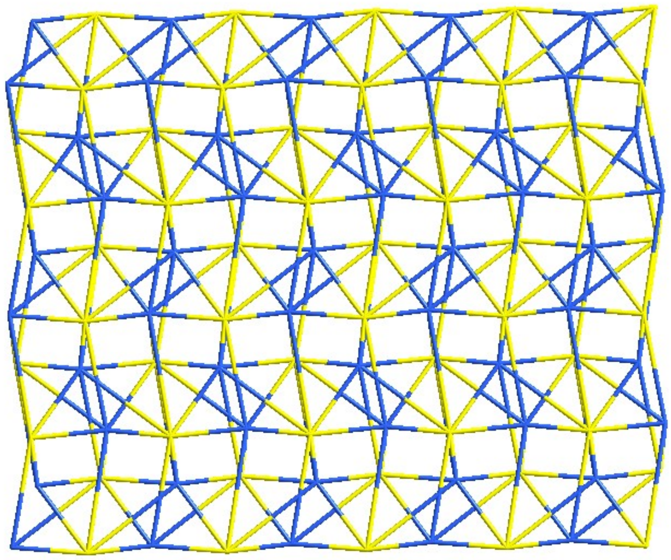

Figure S8   The simplified diagram of 2D-1

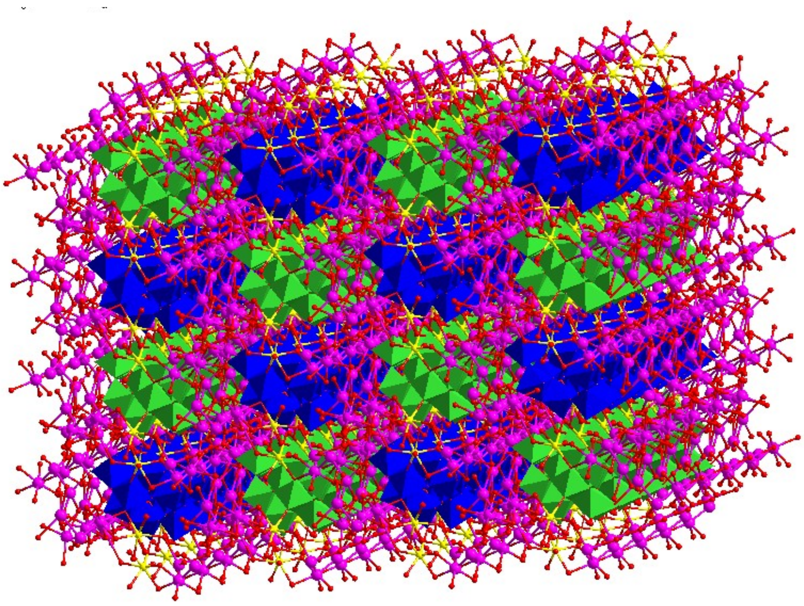

Figure S9 Views of 3D structure of Compound 1

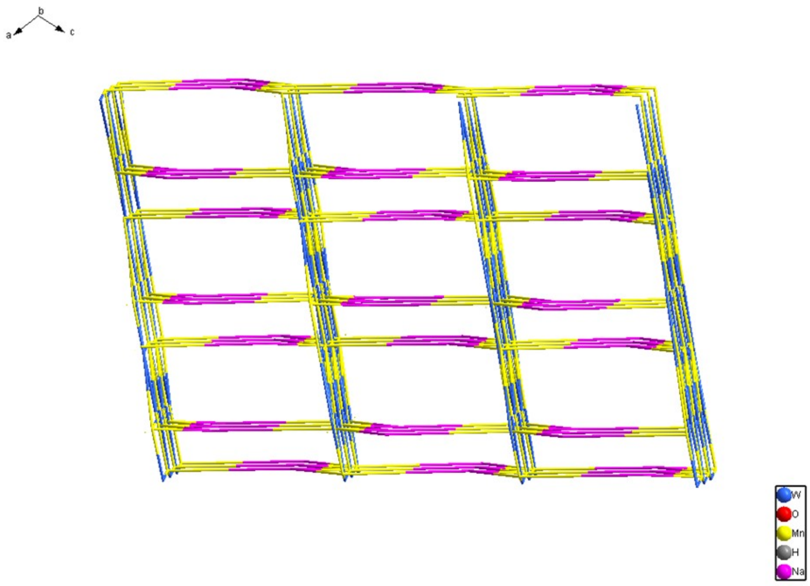

Figure S10 The simplified diagram of 3D

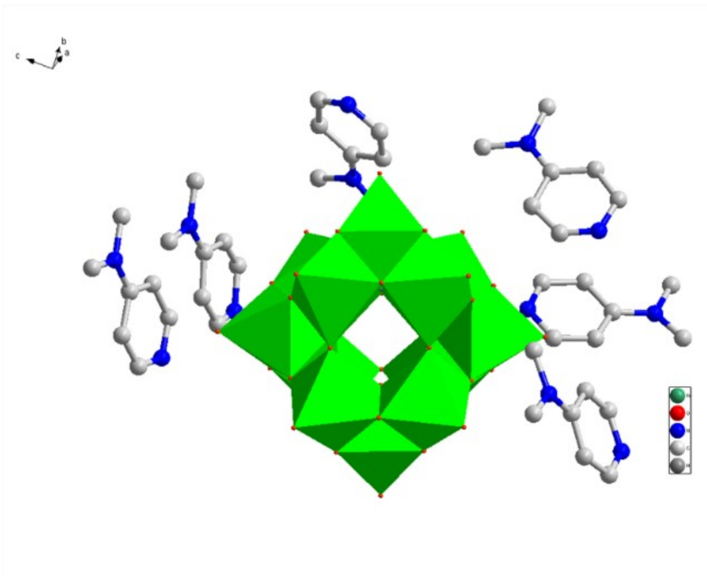

Figure S11 The monomer diagram of Compound 2

(a)

(b)

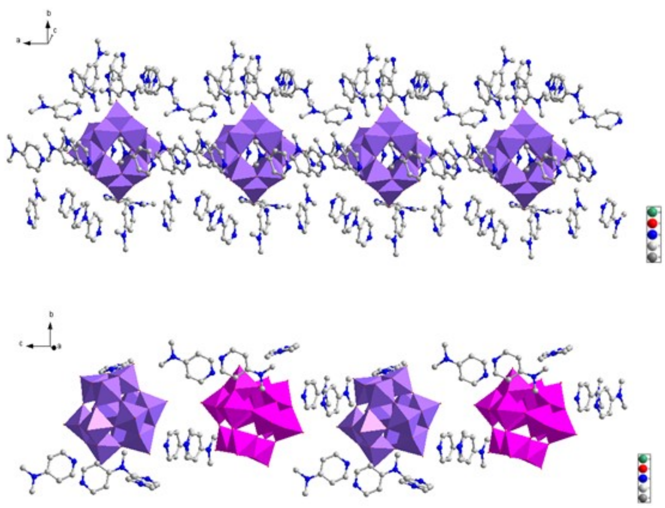

Figure S12 (a) Views of 1D-1 chain structure of Compound 2 (b)Views of 1D-2 chain of Compound 2

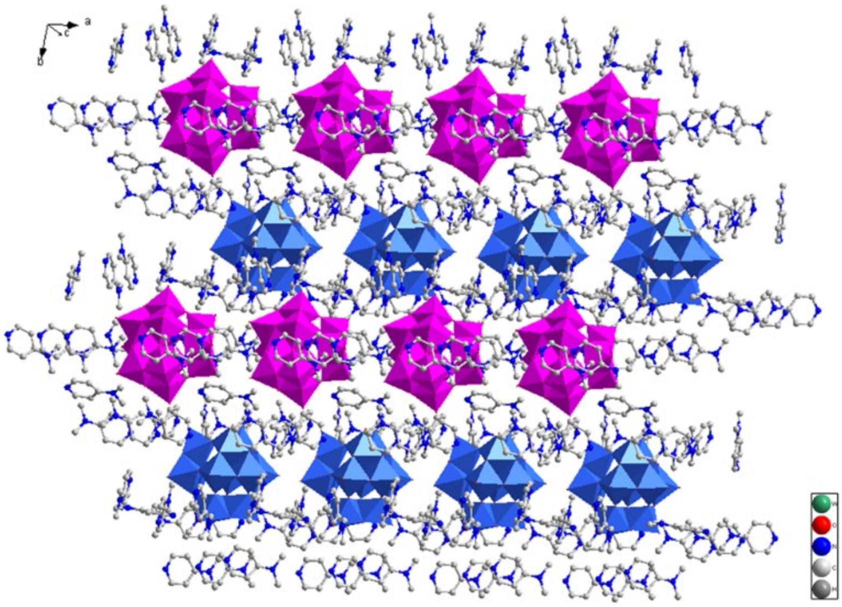

Figure S13 Views of 2D-1 structure of layer structure of Compound 2

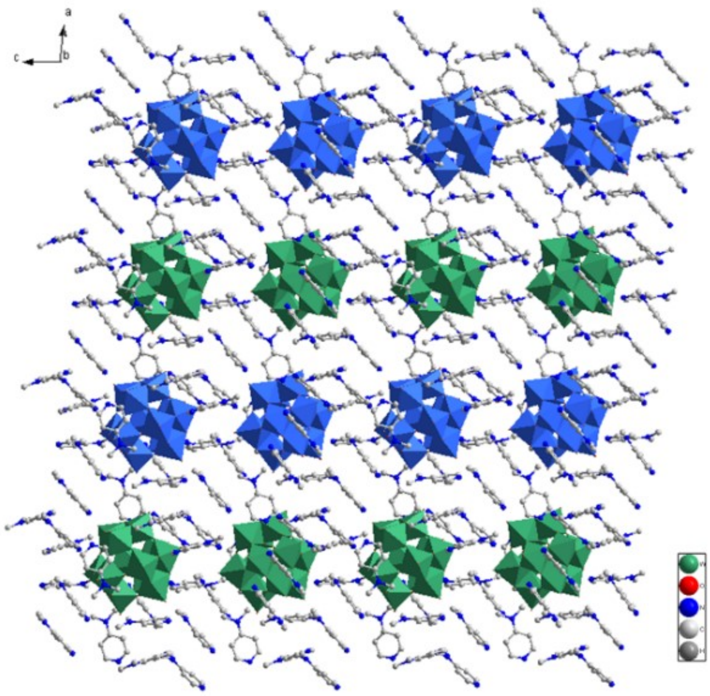

Figure S14 Views of 2D-2 structure of Compound 2

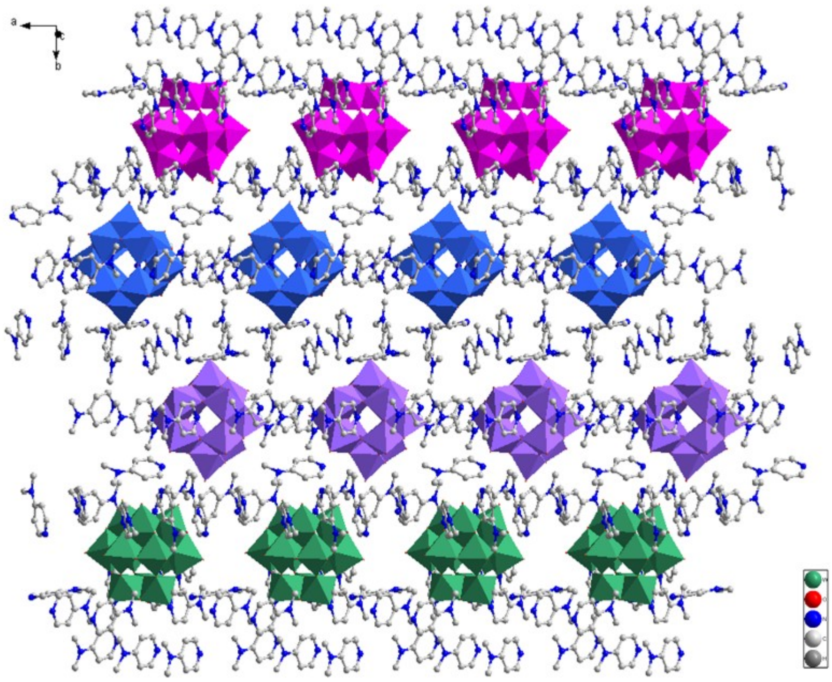

Figure S15 Views of 2D-3 structure of Compound 2

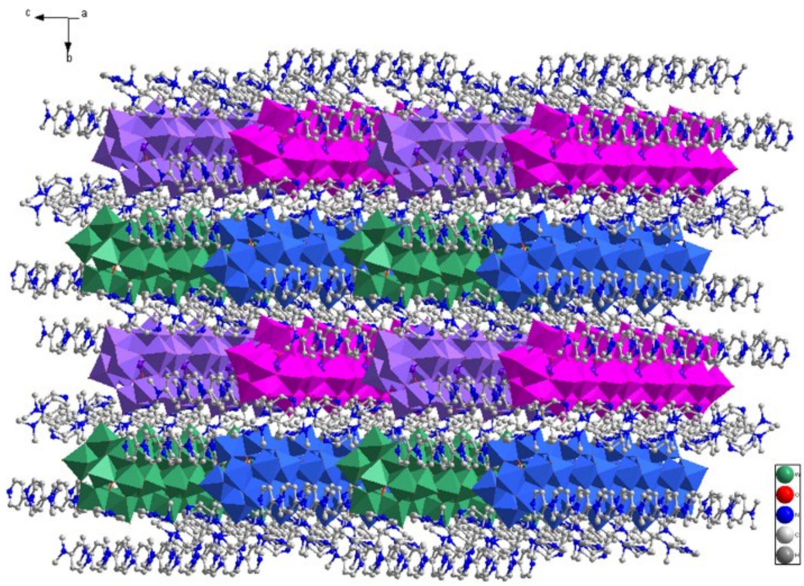

Figure S16 Views of 3D structure of Compound 2

2.3 The characterization diagrams of compounds 1-2

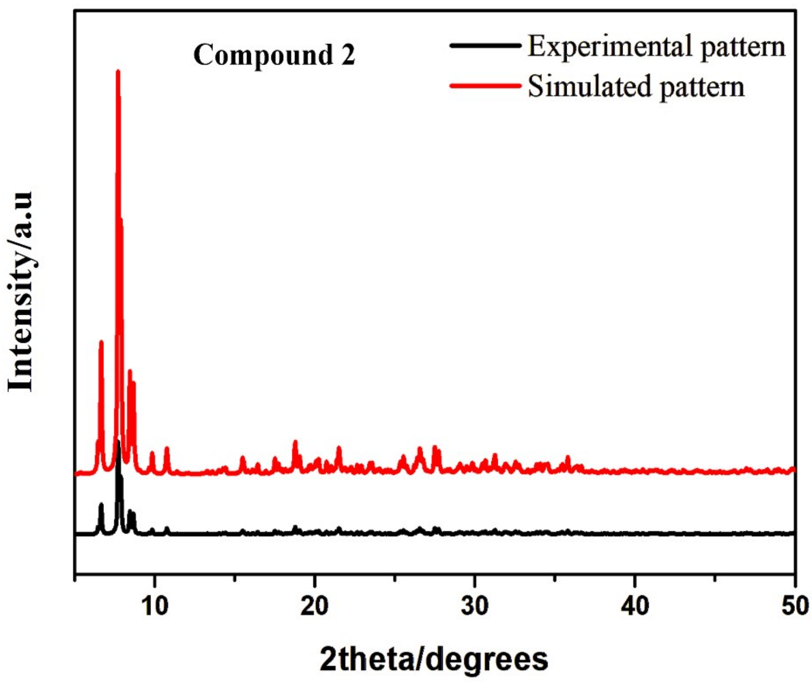

Figure S17 XRD of Compound 2

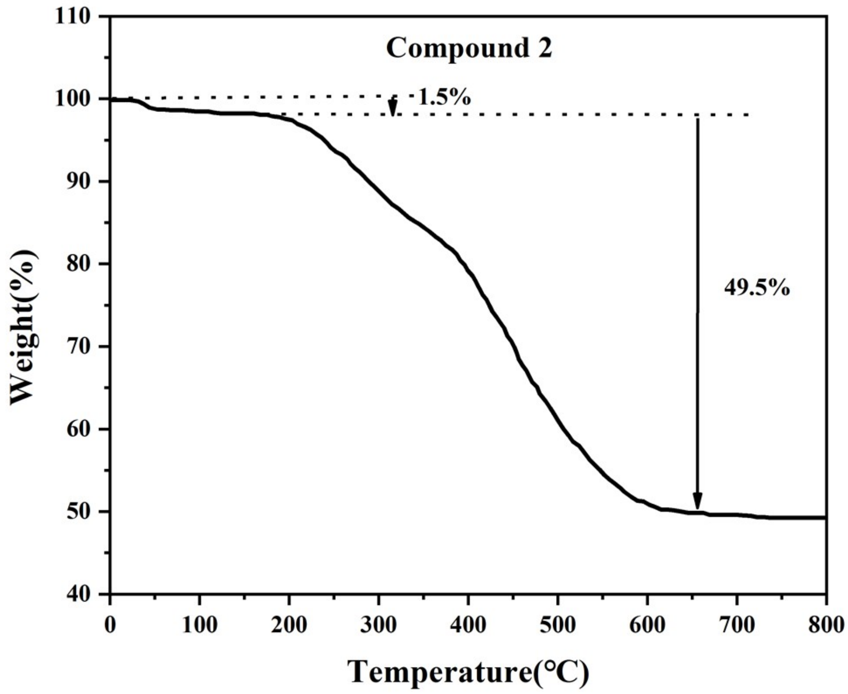

Figure S18 TG of Compound 2

Name	Atomic %
Mn2p	1.38
Na1s	3.87
O1s	36.14
W4f	9.78

Figure S19 The elemental ratio of XPS of Compound 1

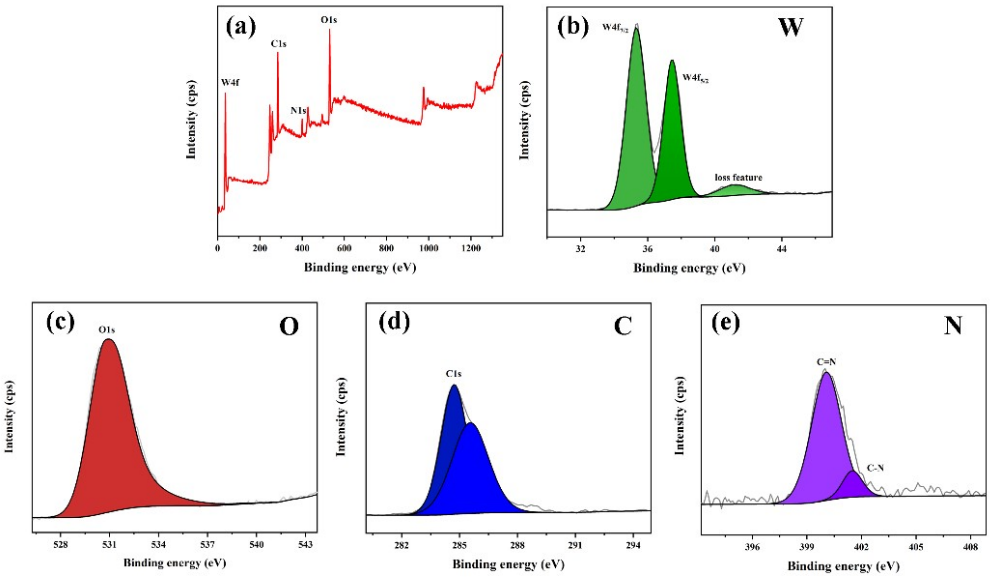

Figure S20 (a)The XPS of Compound 2(b-e) XPS spectra of W4f, O1s, C1s and N1s for Compound 2

Name	Atomic %
C1s	59.57
N1s	7.25
O1s	25.61
W4f	7.34

Figure S21 The elemental ratio of XPS of Compound 2

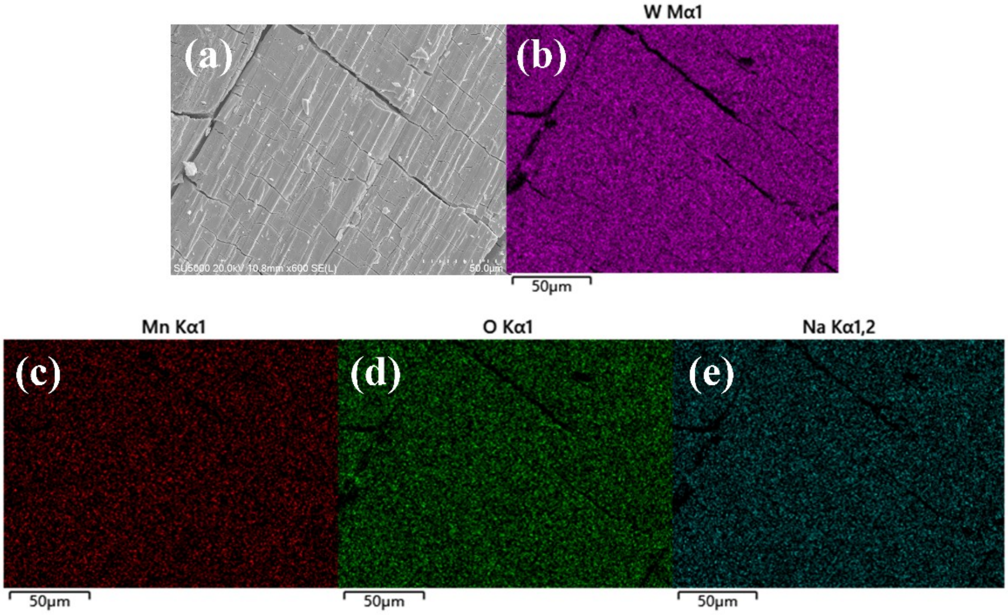

Figure S22 (a)The higher-SEM images of Compound 1 (b-e)The mapping of Compound 1

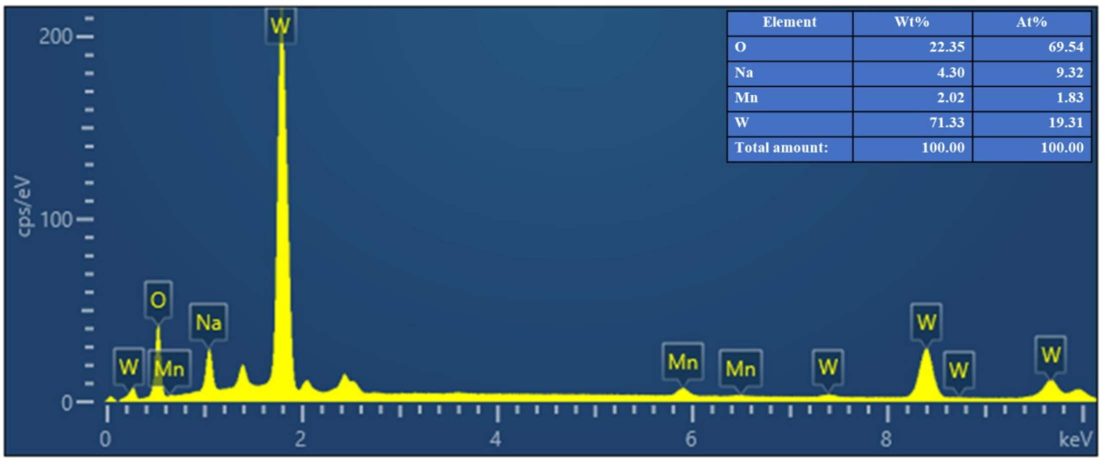

Figure S23 EDS of Compound 1

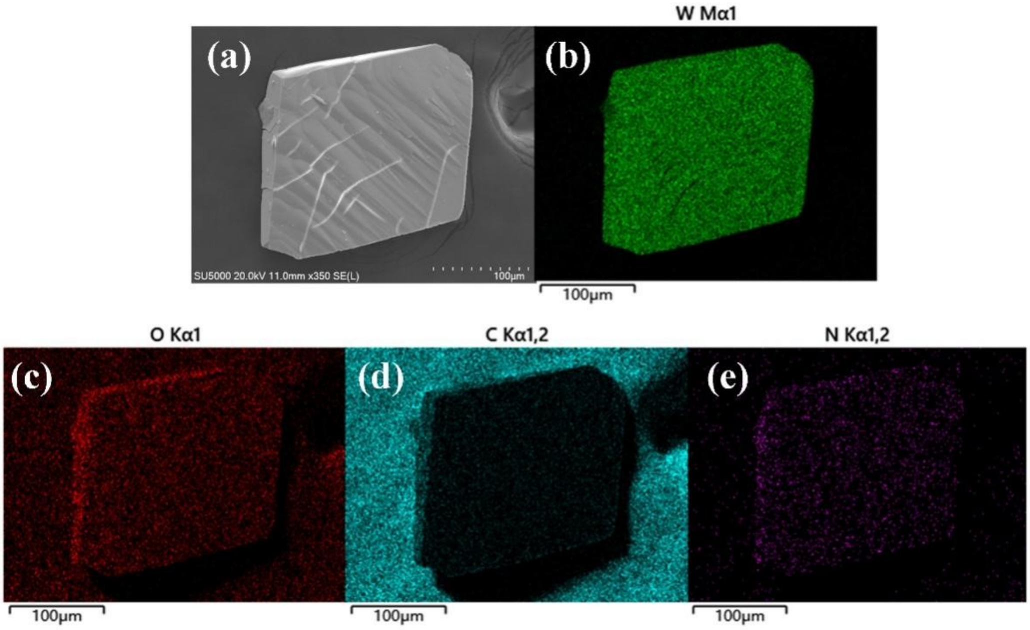

Figure S24(a)The SEM images of Compound 2(b-e)The mapping of Compound 2

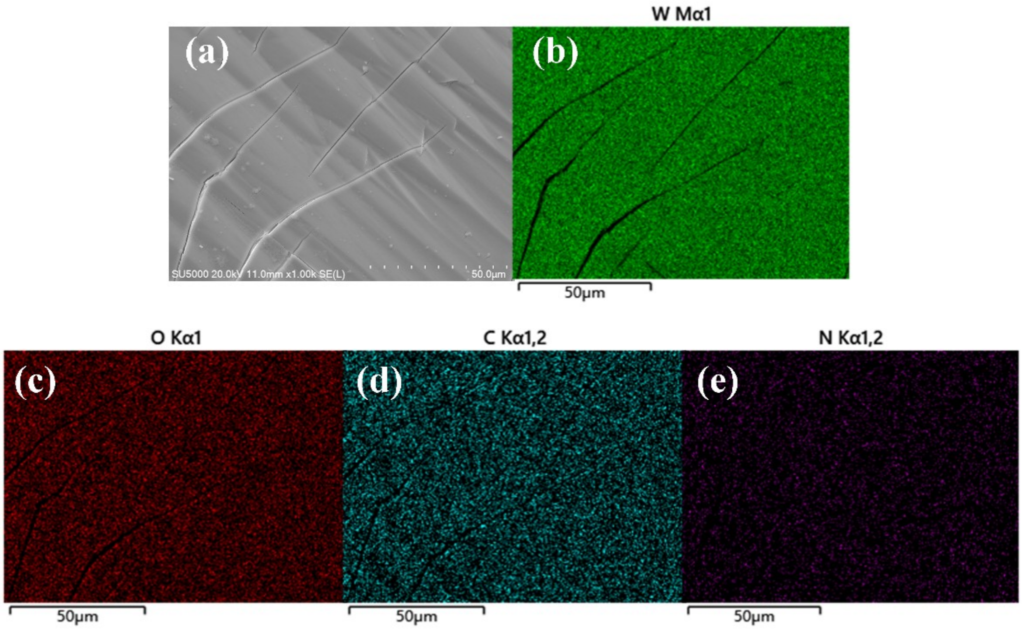

Figure S25 (a)The higher-SEM images of Compound 2 (b-e) The mapping of Compound 2

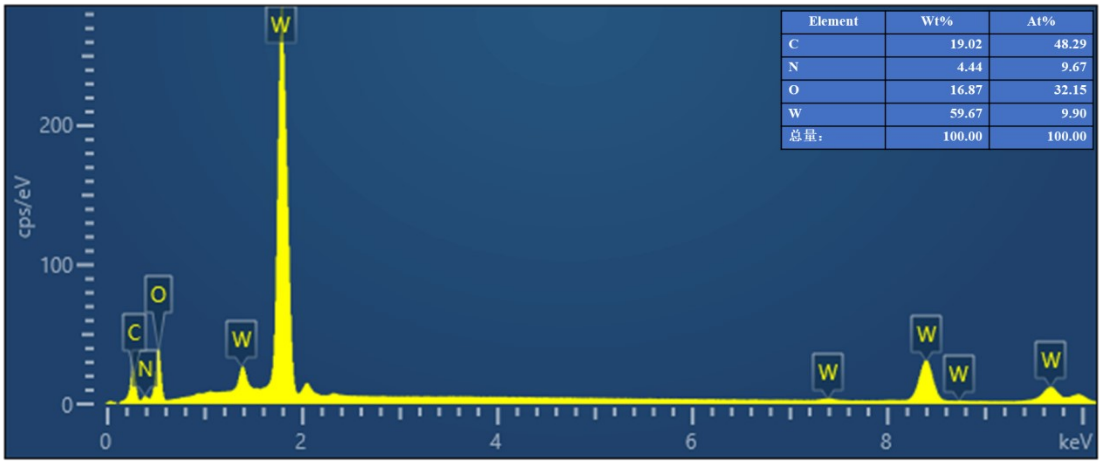

Figure S26 EDS of Compound 2

2.4 BET of Compound 1 and Compound 2

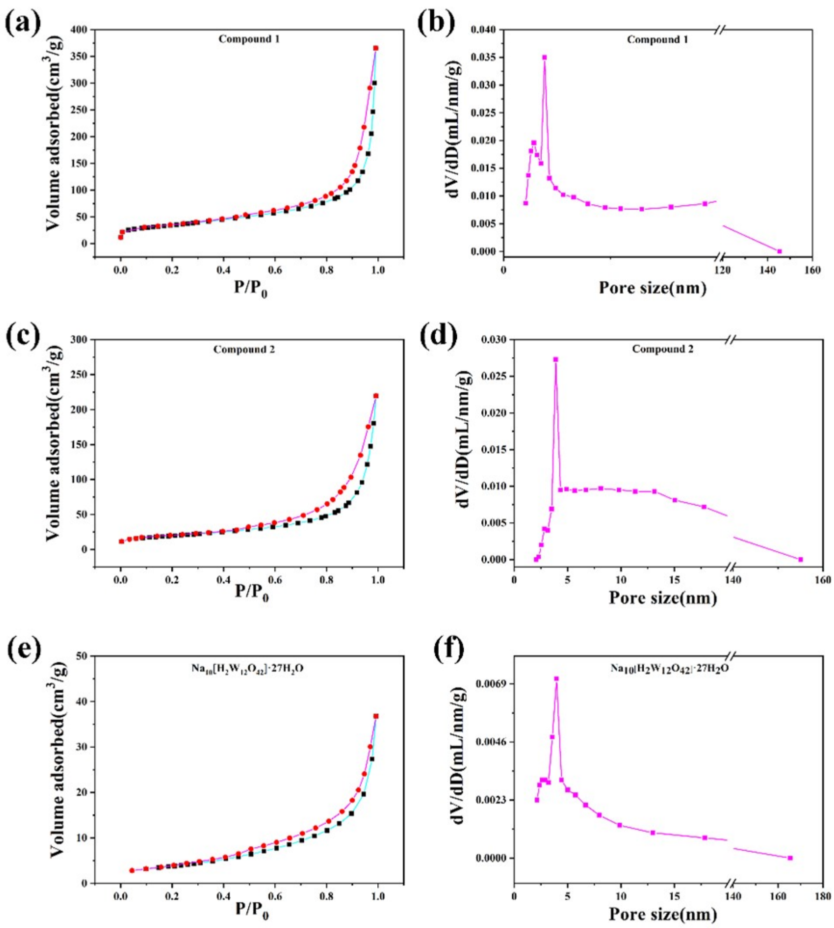

Figure S27 N_2-adsorption–desorption isotherms of (a) Compound 1, (c) Compound 2, (e) $Na_{10}[H_2W_{12}O_{42}]\cdot 27H_2O$;pore size distributions of (b) Compound 1, (d) Compound 2, (f) $Na_{10}[H_2W_{12}O_{42}]\cdot 27H_2O$

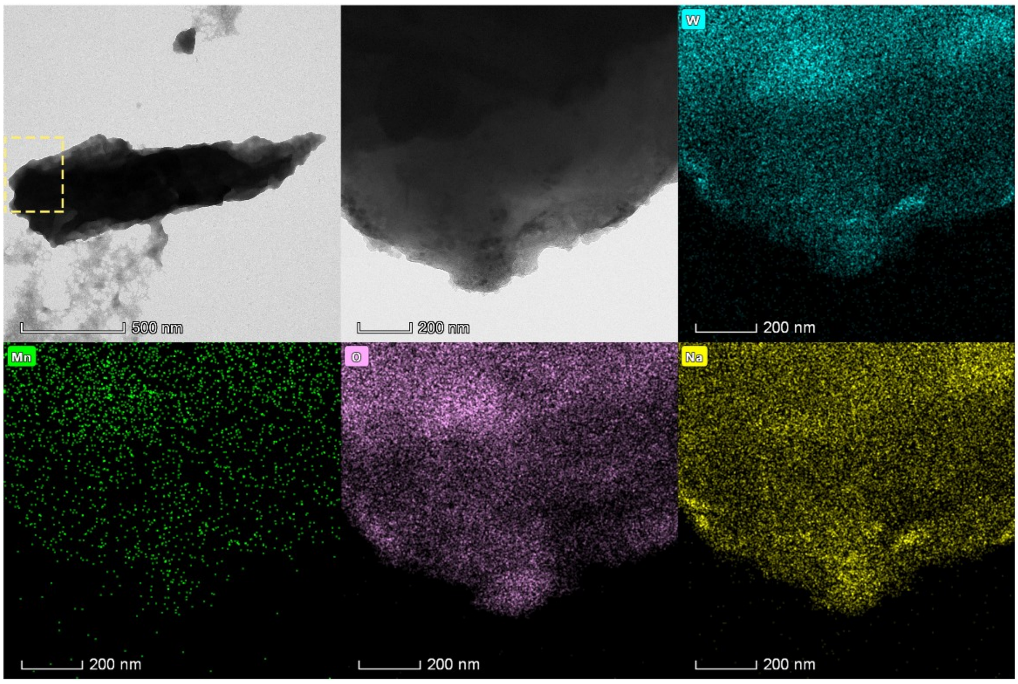

Figure S28 TEM of Compound 1

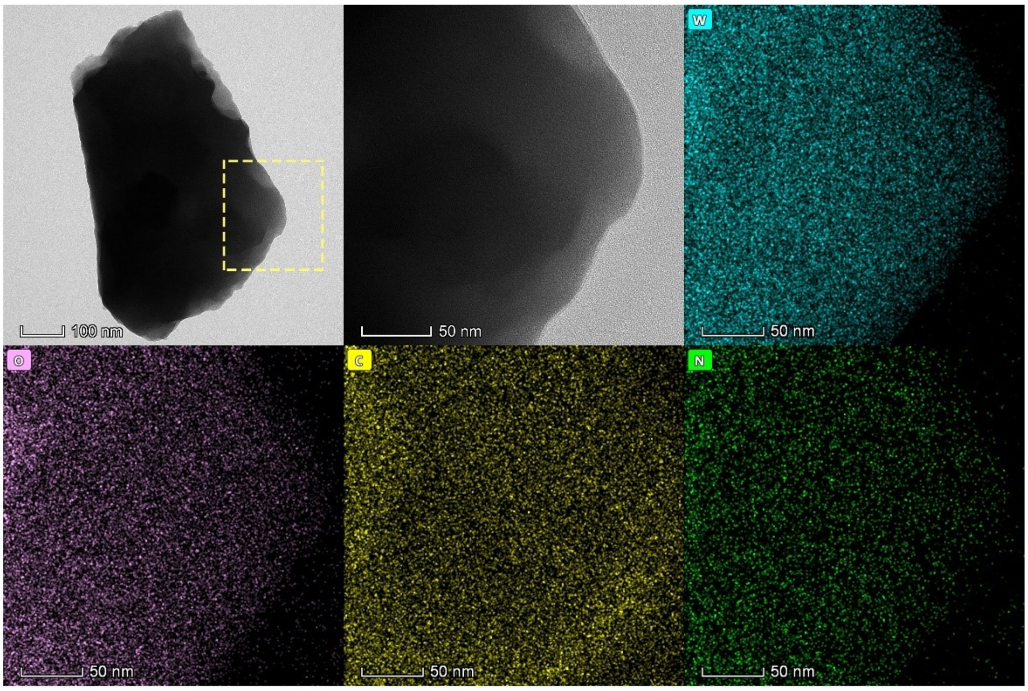

Figure S29 TEM of Compound 2

2.5 HER experiments of Compound 1 and Compound 2 in 0.5 M H_2SO_4

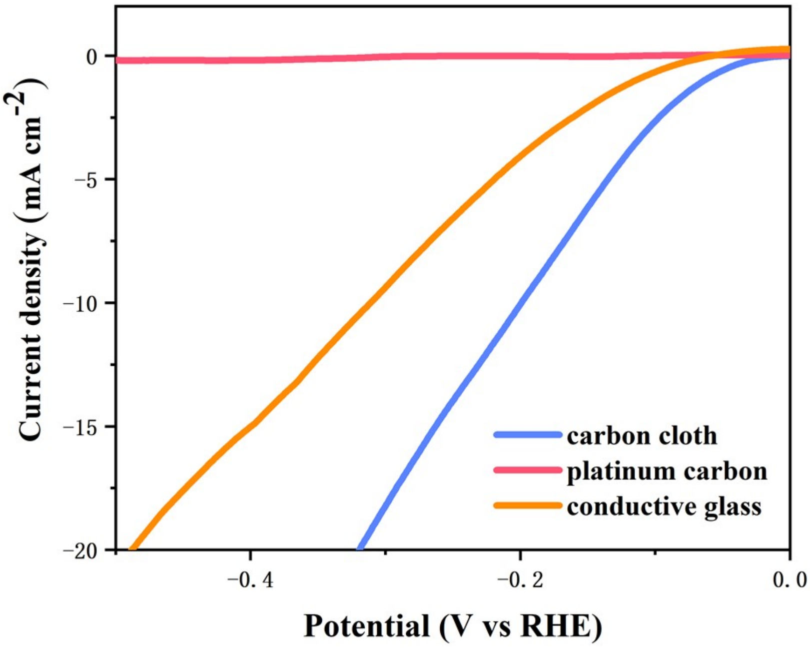

Figure S30 Polarization curves (LSV) of different fluid collectors

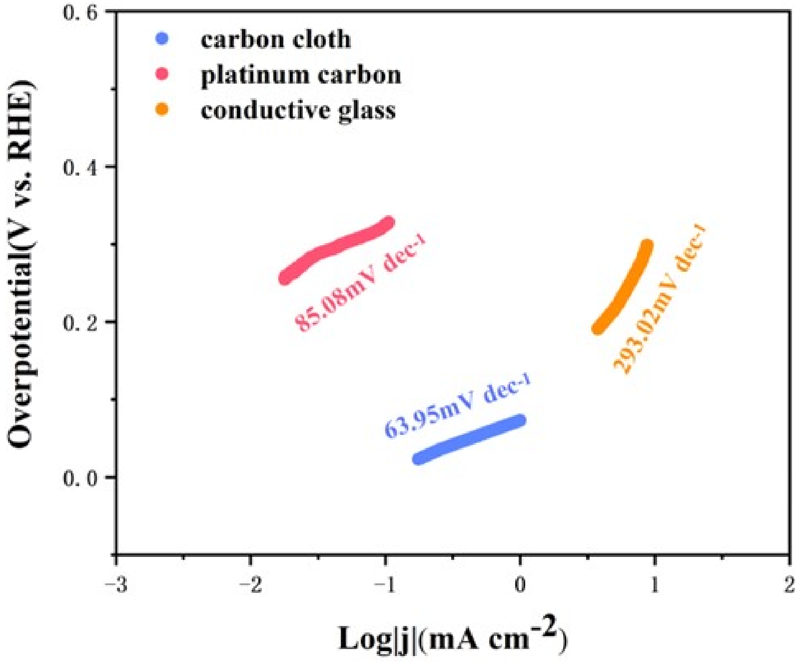

Figure S31 Tafel plots of different fluid collectors

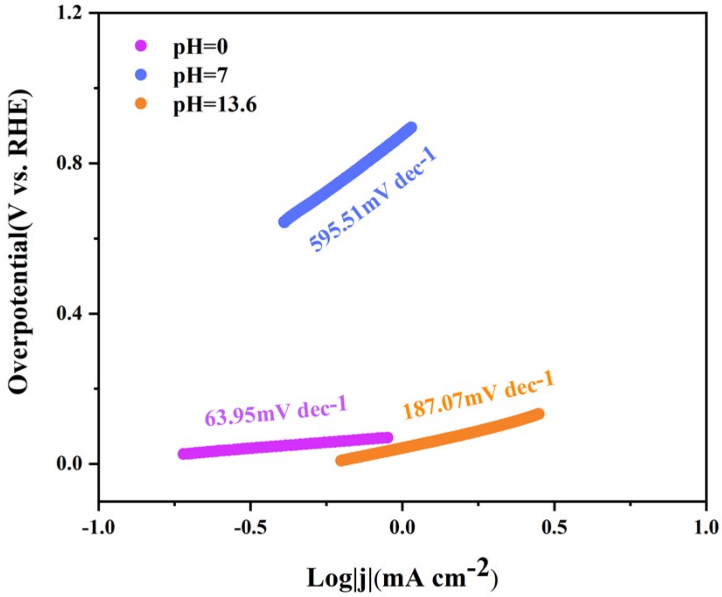

Figure S32 Tafel plots of different pH, measured during HER experiment in 0.5M H_2SO_4 (pH = 0) electrolyte solution

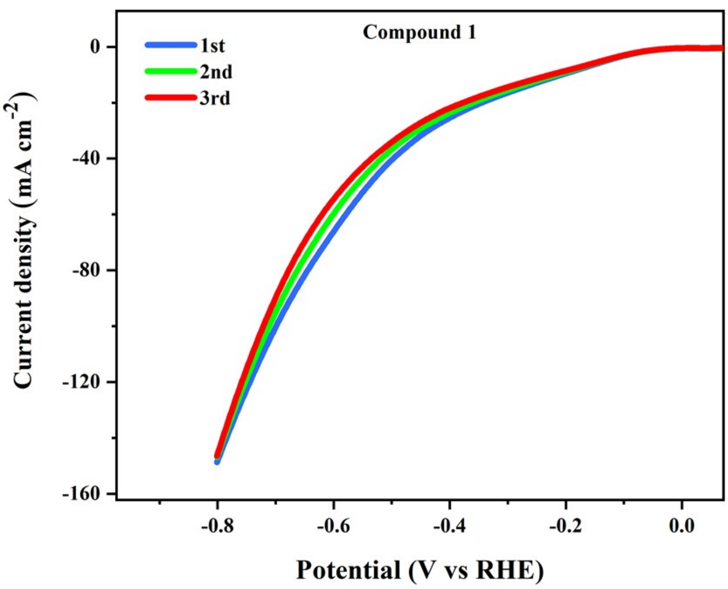

Figure S33 The three LSV curves of Compound 1 for HER test

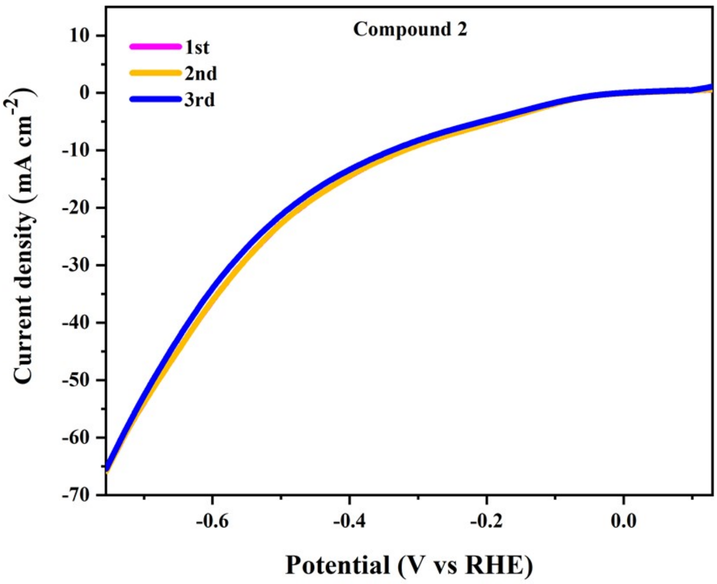

Figure S34 The three LSV curves of Compound 2 for HER test

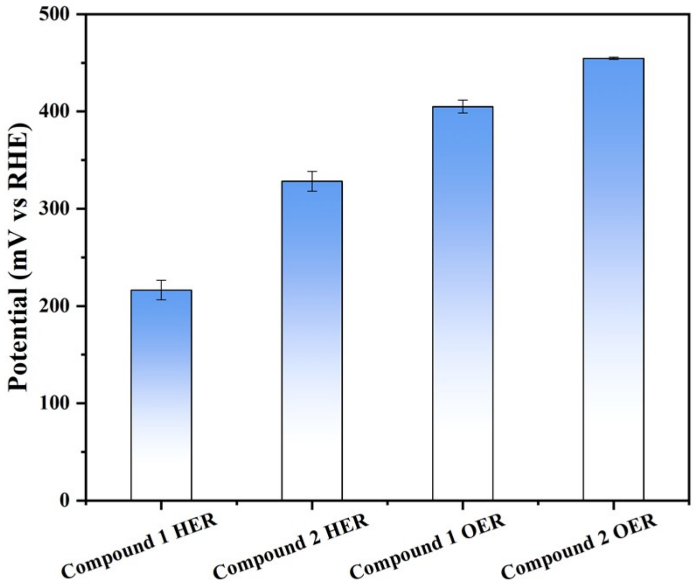

Figure S35 Mean and standard deviation of overpotential values for multiple tests

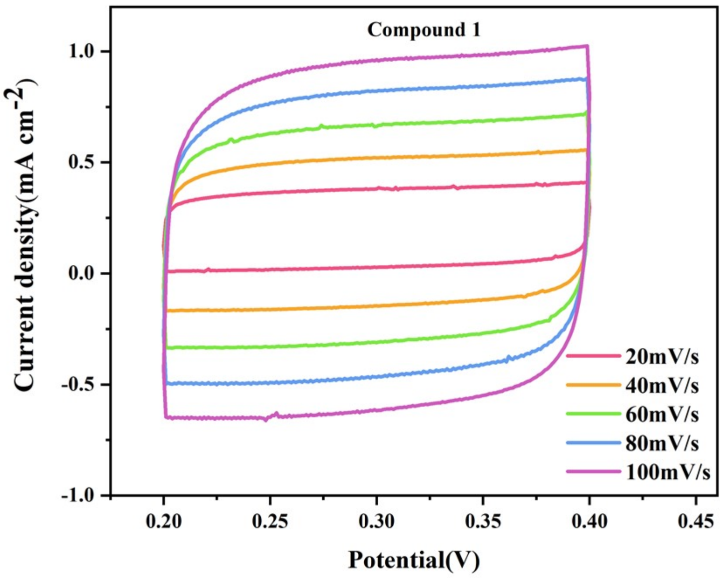

Figure S36 Cyclic voltammetry curves of Compound 1, measured during HER experiment in 0.5M H_2SO_4 (pH = 0) electrolyte solution

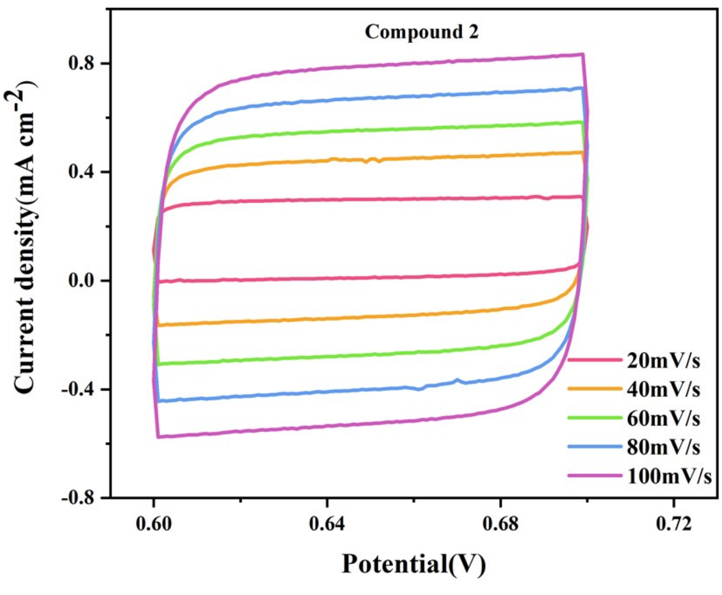

Figure S37 Cyclic voltammetry curves of Compound 2, measured during HER experiment in 0.5M H_2SO_4 (pH = 0) electrolyte solution

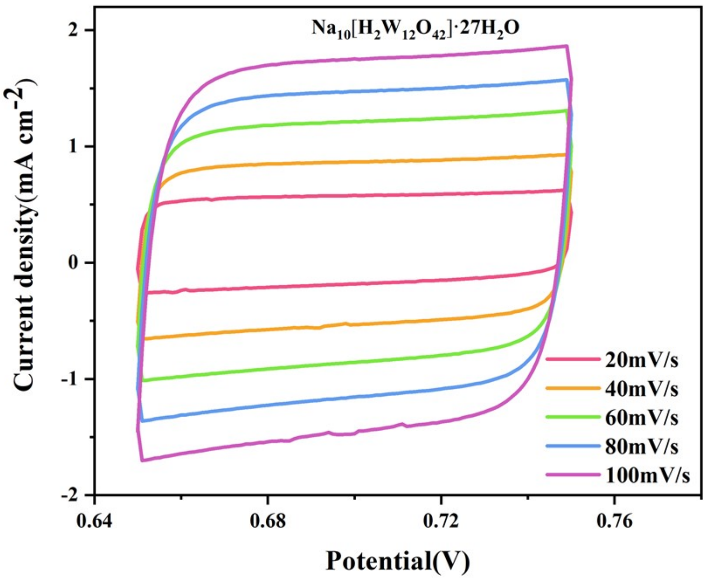

Figure S38 Cyclic voltammetry curves of $Na_{10}[H_2W_{12}O_{42}]\cdot 27H_2O$, measured during HER experiment in 0.5M H_2SO_4 (pH = 0) electrolyte solution

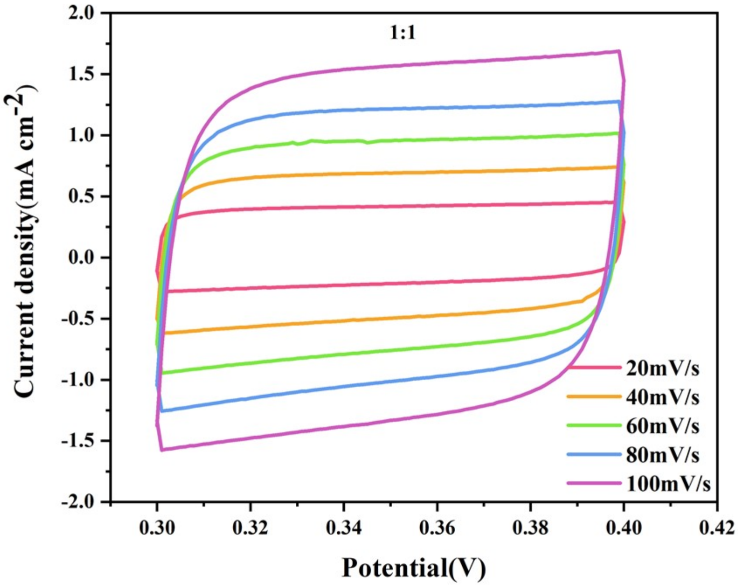

Figure S39 Cyclic voltammetry curves of the ratio of Compound 1 to carbon black is 1:1, measured during HER experiment in 0.5M H_2SO_4 (pH = 0) electrolyte solution

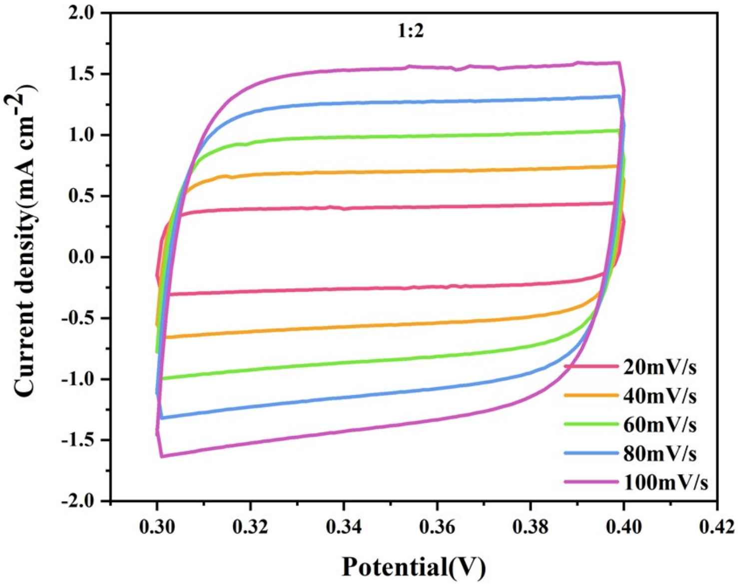

Figure S40 Cyclic voltammetry curves of the ratio of Compound 1 to carbon black is 1:2, measured during HER experiment in 0.5M H_2SO_4 (pH = 0) electrolyte solution

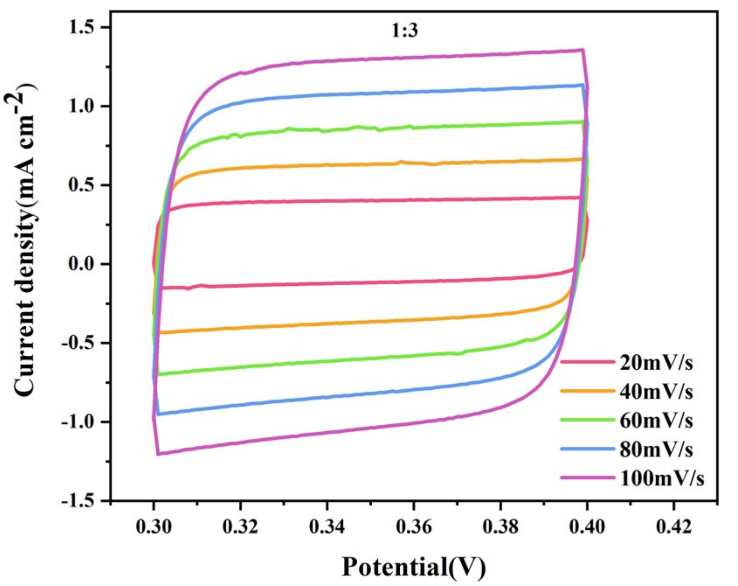

Figure S41 Cyclic voltammetry curves of the ratio of Compound 1 to carbon black is 1:3, measured during HER experiment in 0.5M H_2SO_4 (pH = 0) electrolyte solution

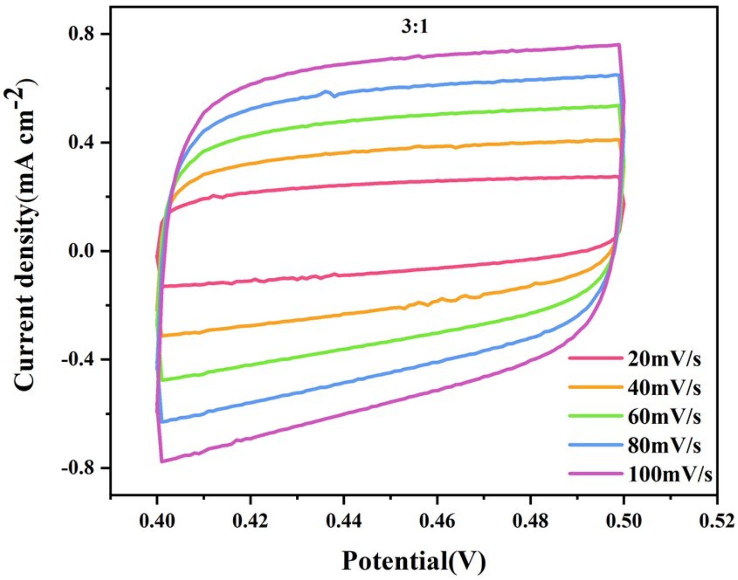

Figure S42 Cyclic voltammetry curves of the different active species / carbon black ratios, measured during HER experiment in 0.5M H_2SO_4 (pH = 0) electrolyte solution

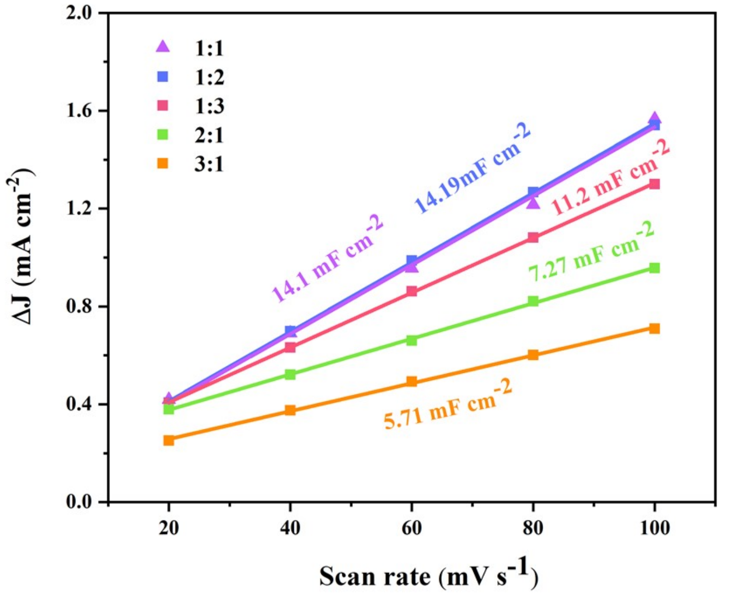

Figure S43 The Cdl of different active species / carbon black ratios measured during HER experiment

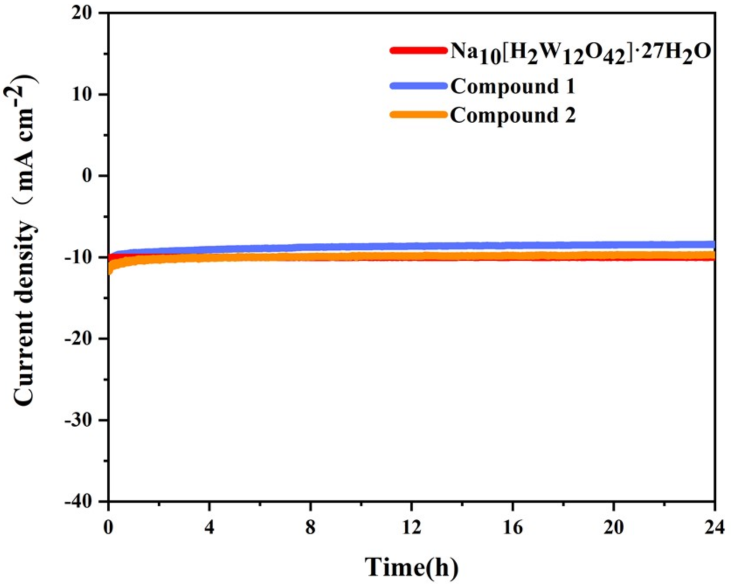

Figure S44 The chronoamperometry curve of different Compounds measured during HER experiment

Table S5 Compare with some polyoxometalates in the literature for HER

HER				Ref
Catalyst	**Electrolyte**	**η_{10}(mV)**	**Tafel slope (mV dec^{-1})**	
NENU-501	0.5 M H_2SO_4	392	137	1
NENU-500 (Polyoxometalate: [e-$Zn_4PMo_8Mo_4O_{40}$])	0.5 M H_2SO_4	237	96	1
NVBO-I	0.5 M H_2SO_4	308	194	2
Cu-W-P/CC (Polyoxometalate: PMo_{12})	0.5 M H_2SO_4	187.4	85.1	4
1D Co(fcdHp)	0.5 M H_2SO_4	450	120	5
[$Cu_2(NL)_2\cdot 4H_2O$] (NTU-33)	0.5 M H_2SO_4	560	158	6
H_8L-Co-Crystal MOF	0.5 M H_2SO_4	234	102	7
MoP	0.5 M H_2SO_4	297	82	3
POM-MoP (Polyoxometalate: $PMO_{12}O_{40}$)	0.5 M H_2SO_4	198	80	3
NVBO-I	0.5 M H_2SO_4	308	194	2
[H_2TETA][Ni(H_2 hedp)$_2$]$\cdot 2H_2O$	0.5 M H_2SO_4	398	232	10
HPOM-MoP/C (Polyoxometalate: $PMO_{12}O_{40}$)	0.5 M H_2SO_4	187	55	16
POM@ZnCoS/NF (Polyoxometalate: PW_{12})	1 M KOH	170	535	8
POM =PW_{12}	1 M KOH	240	___	8
ZnCo DHNWs	1 M KOH	227	120.5	8
ZnCoS NWs	1 M KOH	206	108.6	8
Cu_3P/CuP_2/CC {HKUST-1}	0.5 M H_2SO_4	266.1	86.9	18
MoP/CC (Polyoxometalate: PMo_{12})	0.5 M H_2SO_4	223.6	74.2	18
Cu-W-P/CC (Polyoxometalate: PMo_{12})	0.5 M H_2SO_4	187.4	85.1	18
CoS_2-MoS_2	0.5 M H_2SO_4	220	64.2	17

Mn/oMA-PW/RCPE	1 M KOH	380	111	22
$WSe_2/Co_{0.85}Se$/graphene	0.5 M H_2SO_4	217	64	23
POM@Ni-MOF	0.5 M H_2SO_4	68	77.3	27
Co_9S_8@MoS2 (Polyoxometalate: PMo_{12})	1M KOH	230	84	28
$NiCo_2S_4$/PANI@POM/rGO (Polyoxometalate:$PW_{12}O_{40}$)	1M KOH	197	47.5	29
RuPOM/KB (Polyoxometalate: $SiW_{10}O_{36}$)	Seawater (pH 8.1)	760	——	30
Ni-Mo_2C/NPC (Polyoxometalate: $(NH_4)_4[NiMo_6O_{24}H_6]$)	1.0 M KOH	183	64	31
Co_4Mo_2@NC (Polyoxometalate: $(NH_4)_6Mo_7O_{24}\cdot 4H_2O$)	1.0 M KOH	∽218	73.5	32
HC800 (Polyoxometalate: $(NH_4)_6Mo_7O_{24}\cdot 4H_2O$)	0.5 M H_2SO_4	192	98	33
SL-MoS2-CNT (Polyoxometalate: $(NH_4)_6Mo_7O_{24}$)	0.1 M H_2SO_4	236	63	34
CoMoS-600 (Polyoxometalate:$H_3PMo_{12}O_{40}x\cdot H_2O$)	0.5 M H_2SO_4	235	65.5	35

2.6 OER experiments of Compound 1 and Compound 2 in 0.5 M KOH

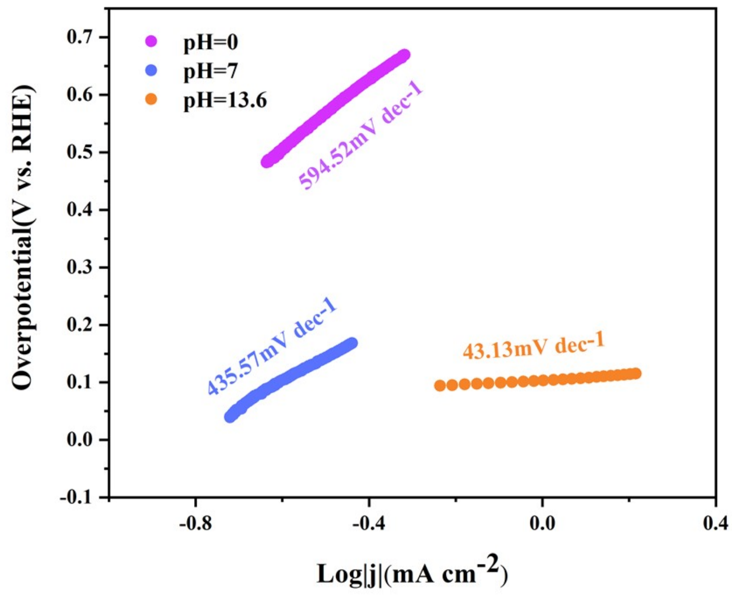

Figure S45 Tafel plots of different pH, measured during OER experiment in 0.5M KOH (pH = 13.6) electrolyte solution

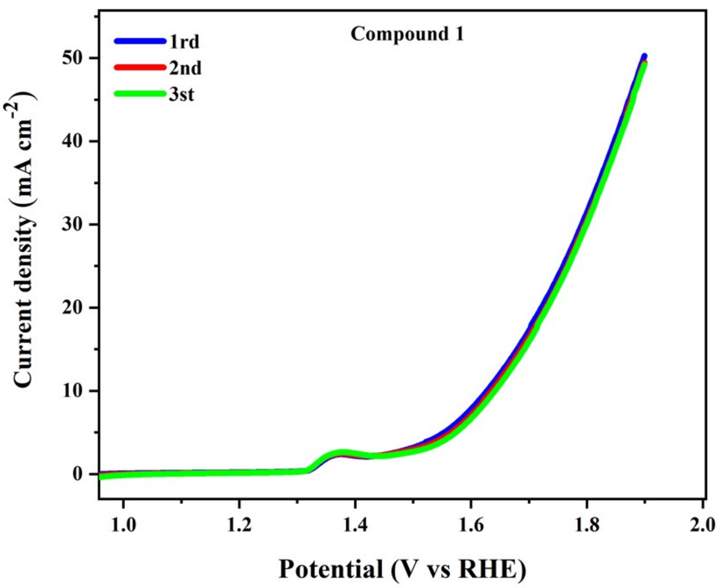

Figure S46 The three LSV curves of Compound 1 for OER test

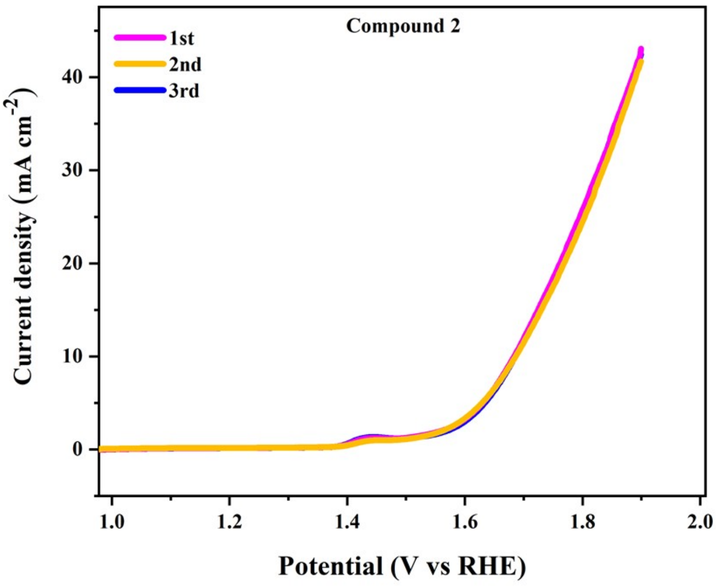

Figure S47 The three LSV curves of Compound 2 for OER test

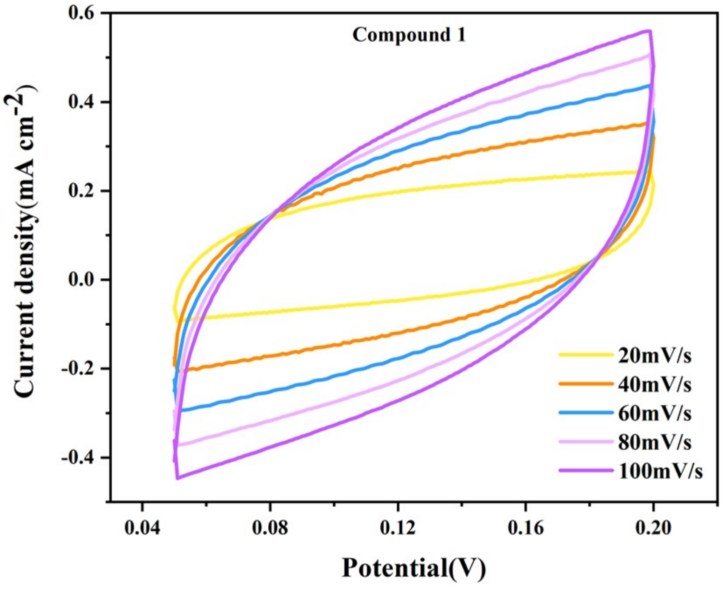

Figure S48 Cyclic voltammetry curves of Compound 1, measured during OER experiment in 0.5M KOH (pH = 13.6) electrolyte solution

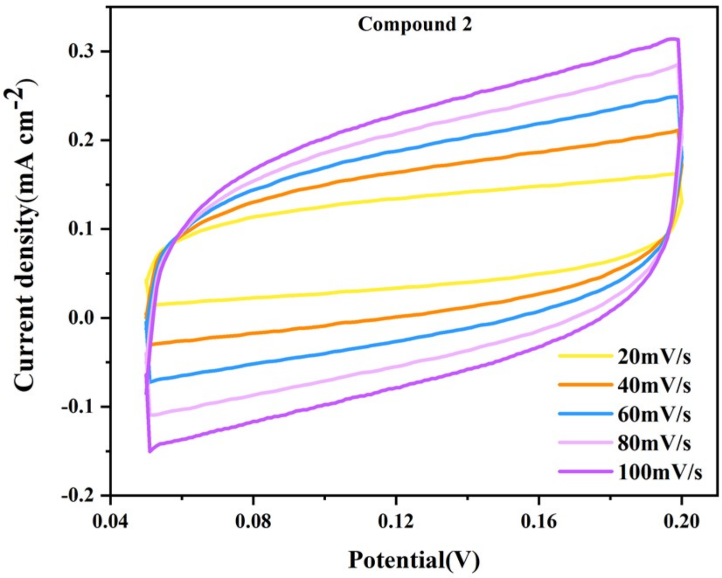

Figure S49 Cyclic voltammetry curves of Compound 2, measured during OER experiment in 0.5M KOH (pH = 13.6) electrolyte solution

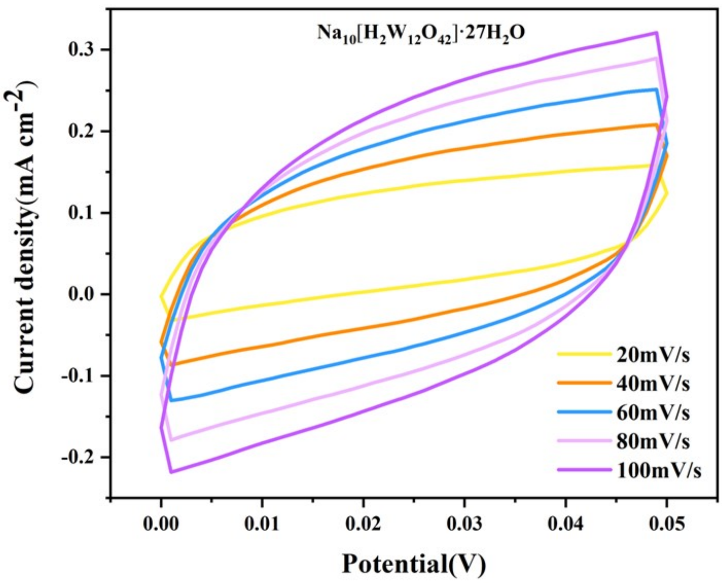

Figure S50 Cyclic voltammetry curves of $Na_{10}[H_2W_{12}O_{42}]$ $27H_2O$, measured during OER experiment in 0.5M KOH (pH = 13.6) electrolyte solution

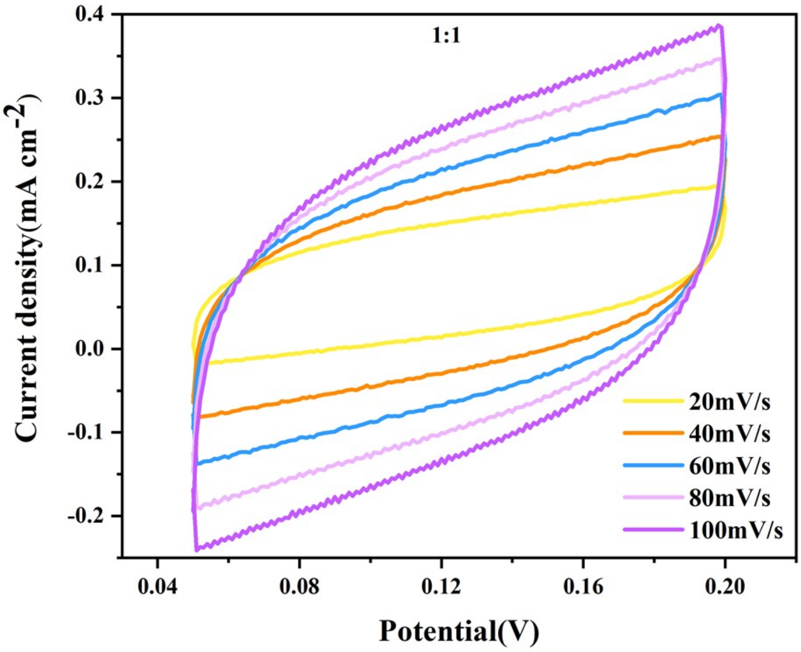

Figure S51 Cyclic voltammetry curves of the ratio of Compound 1 to carbon black is 1:1, measured during OER experiment in 0.5M KOH(pH = 13.6) electrolyte solution

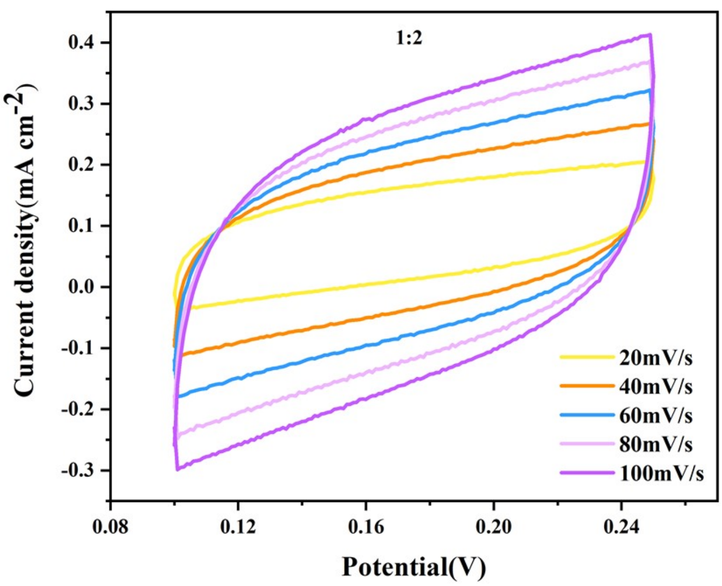

Figure S52 Cyclic voltammetry curves of the ratio of Compound 1 to carbon black is 1:2, measured during OER experiment in 0.5M KOH(pH = 13.6) electrolyte solution

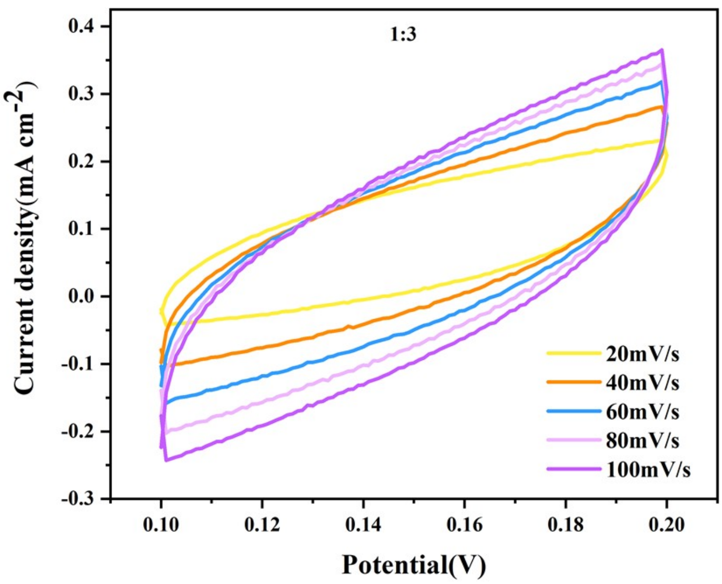

Figure S53 Cyclic voltammetry curves of the ratio of Compound 1 to carbon black is 1:3, measured during OER experiment in 0.5M KOH(pH = 13.6) electrolyte solution

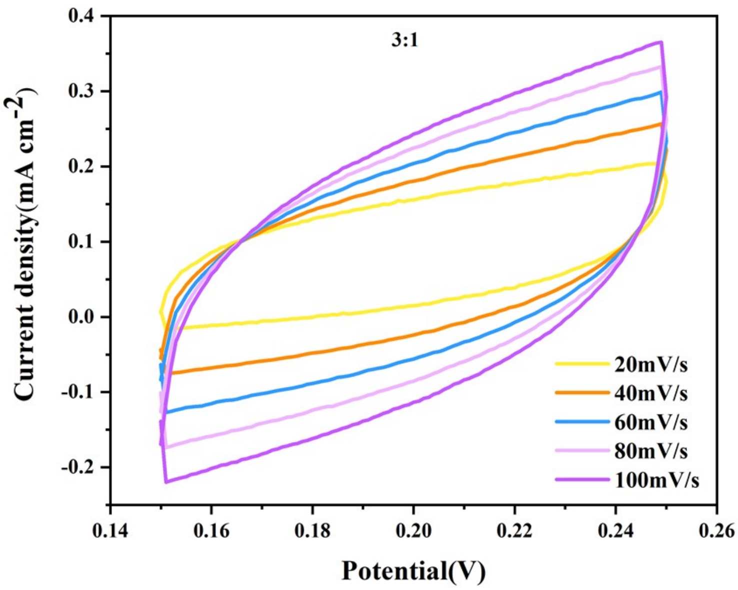

Figure S54 Cyclic voltammetry curves of the ratio of Compound 1 to carbon black is 3:1; measured during OER experiment in 0.5M KOH(pH = 13.6) electrolyte solution

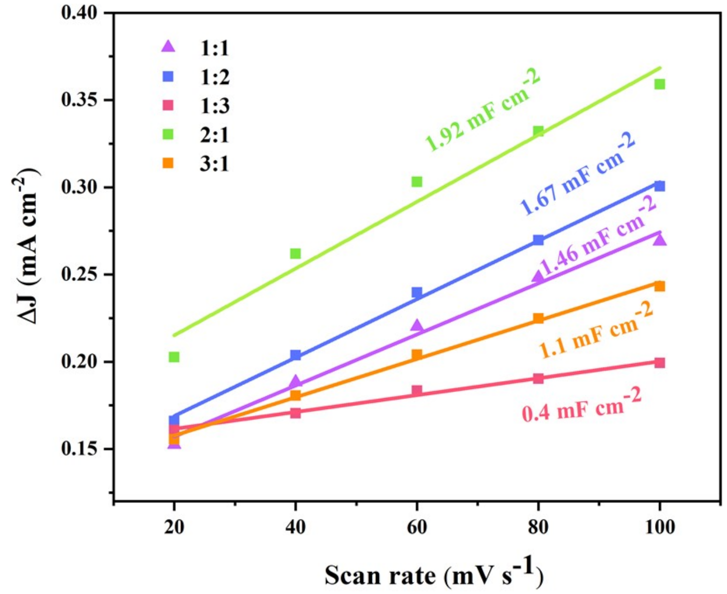

Figure S55 The Cdl of different active species / carbon black ratios measured during OER experiment

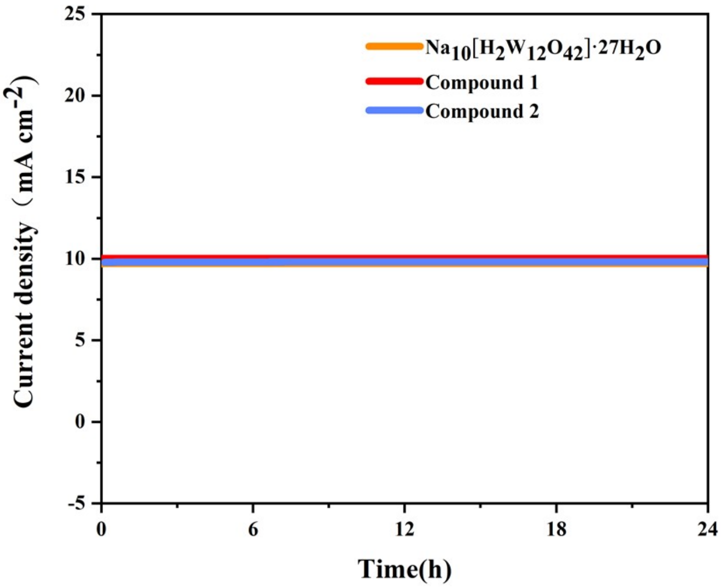

Figure S56 The chronoamperometry curve of different Compounds measured during OER experiment

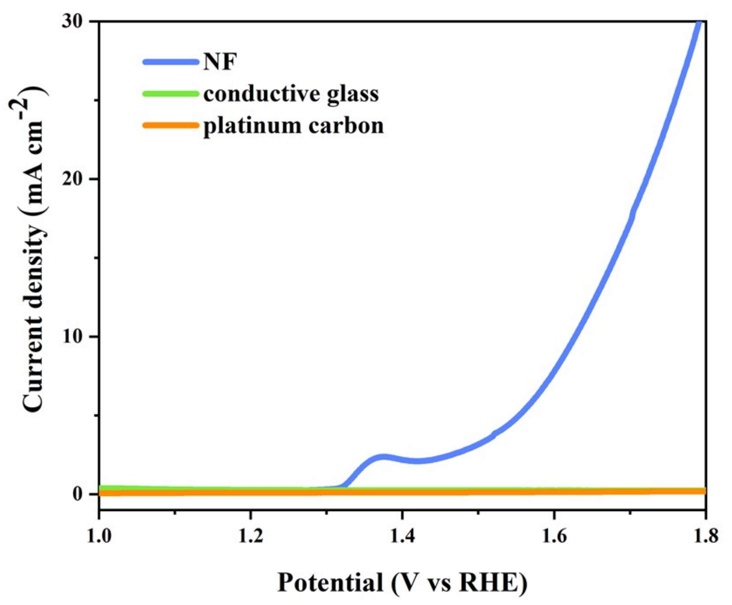

Figure S57 Polarization curves (LSV) of different fluid collectors(OER)

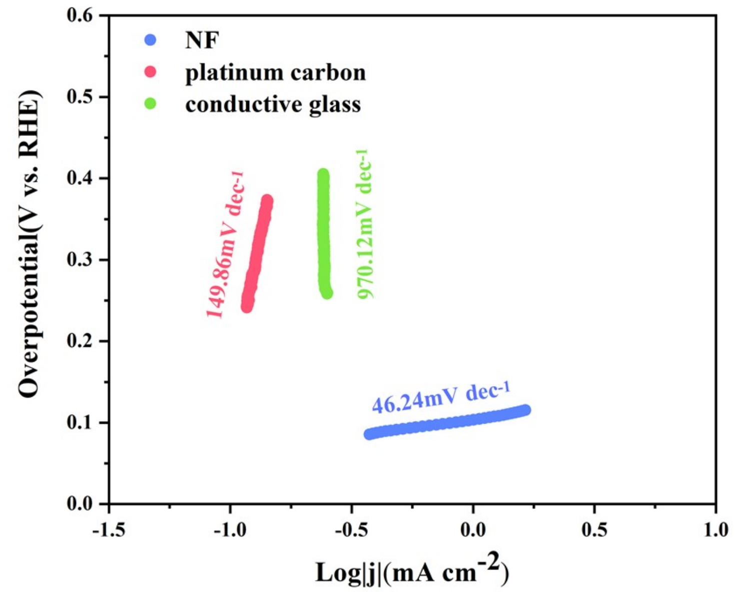

Figure S58 Tafel plots of different fluid collectors

Table S6 Compare with some polyoxometalates in the literature for OER

OER				Ref
Catalyst	**Electrolyte**	**η_{10}(mV)**	**Tafel slope (mV dec^{-1})**	
CoP/C	0.1 M KOH	360	——	8
$Mn_3O_4/CoSe_2$	0.1 M KOH	450	——	8
$CoC_2O_4{\cdot}2H_2O$	0.1 M KOH	436	——	8
Ni-Co-LDH/Ni foam	0.1 M KOH	420	——	8
FeNi@NC	1 M KOH	390	81	9
NH_4VO_3	1 M KOH	532	___	2
H_3BO_3	1 M KOH	702	___	2
$Na_2B_4O_7{\cdot}10H_2O$	1 M KOH	561	___	2
Co_2B-500	1 M KOH	380	45	11
NiPc-Ni	1 M KOH	427	83	12
P_1(PBA@POM(0.01g)) (Polyoxometalate:$H_3PMo_{12}O_{40}$)	1 M KOH	580	55.69	13
P_2 (PBA@POM(0.1g)) (Polyoxometalate:$H_3PMo_{12}O_{40}$)	1 M KOH	560	44.21	13
P_3(PBA@POM(1g)) (Polyoxometalate: $H_3PMo_{12}O_{40}$)	1 M KOH	440	23.45	13
P_4(PBA@POM(2g)) (Polyoxometalate: $H_3PMo_{12}O_{40}$)	1 M KOH	540	42.65	13
SiW_9Co_3@ZIF-67	0.1 M KOH	470	113.6	14
MnVOx@NrGO (1-400)	0.1 M KOH	440	286	15
MnVOx@NrGO (1-900)	0.1 M KOH	420	271	15
Fe-POM	1 M KOH	434	87	27
Ni-$\{P_4Mo_6\}$	1 M KOH	320	67	28
$Ba_{14}[\{FeCo_3(OH)_3PO_4\}_4(SiW_9O_{34})_4]$	1 M H_2SO_4	398	___	29
MnFe-oxide	0.1 M KOH	720	80	24

$MnFe_2O_4$	0.1 M KOH	582	71	25
MnOx-10	1 M KOH	393	84	26
POM@Ni-MOF	1 M KOH	107.3	61	27
([PVIM][V-Co_4]) (Polyoxometalate: Co-WCo_3)	1 M KOH	430	___	36
PW_{12}@amZIF (Polyoxometalate: $PNiOW_{11}$)	1 M KOH	423	86	37

2.7 Summary of HER and OER performance for the work in this paper

Table S7 Summary of HER and OER performance for the work in this paper

HER				
Catalyst	**Electrolyte**	**pH**	**Overpotential (η) at 10 mA cm^{-2}**	**Tafel slope ($mV\ dec^{-1}$)**
Compound 1(2:1)	0.5 M H_2SO_4	0	199	63.95
Compound 2	0.5 M H_2SO_4	0	322	78.86
$Na_{10}[H_2W_{12}O_{42}]·27H_2O$	0.5 M H_2SO_4	0	440	495.76
Bare carbon cloth	0.5 M H_2SO_4	0	552	46.6
Pt/C	0.5 M H_2SO_4	0	108	66.7
Compound 1(1:1)	0.5 M H_2SO_4	0	271	116.36
Compound 1(1:2)	0.5 M H_2SO_4	0	373	133.45
Compound 1(1:3)	0.5 M H_2SO_4	0	412	138
Compound 1(3:1)	0.5 M H_2SO_4	0	498	184.52
Compound 1(2:1)	1 M PBS	7	——	595.51
Compound 1(2:1)	0.5 M KOH	13.6	——	187.01
OER				
Catalyst	Electrolyte	pH	Overpotential (η) at 10 mA cm^{-2}	Tafel slope ($mV\ dec^{-1}$)
Compound 1(2:1)	0.5 M KOH	13.6	398	46.24
Compound 2	0.5 M KOH	13.6	447.4	80.41
$Na_{10}[H_2W_{12}O_{42}]·27H_2O$	0.5 M KOH	13.6	496.4	81.09
Bare NF	0.5 M KOH	13.6	541.4	85.92

RuO_2	0.5 M KOH	13.6	314.4	132.26
Compound 1(1:1)	0.5 M KOH	13.6	436.4	137.85
Compound 1(1:2)	0.5 M KOH	13.6	443	134.36
Compound 1(1:3)	0.5 M KOH	13.6	417.4	111.19
Compound 1(3:1)	0.5 M KOH	13.6	490.4	157.12
Compound 1(2:1)	1 M PBS	7	——	435.57
Compound 1(2:1)	0.5 M H_2SO_4	0	——	594.52

2.8 Determination of Turn Over Frequency (TOF)

The exhaust method is used to obtain the yield of H_2 and O_2, and the relevant content for determining the content of H_2 and O_2.

The TOF value for HER and OER experiments can be calculated as described equation

$$TOF = \frac{j\,N_A}{Fn\Gamma}$$

Where,

j = current density (mA cm^{-2}),N_A = Avogadro constant (6.0221×10^{-23}) mol^{-1}, n is the number of electrons transferred = 2, Γ is the surface or total concentration of catalyst in terms of number of atoms.

Surface area of carbon cloth = 2cm^2

Molar mass of $Na_{12}H_6[Mn_2W_{12}O_{43}(H_2O)_8(OH)_8]\cdot 8H_2O$ = 3694.08g

Mass contribution of Mn atoms in 1 mole $Na_{12}H_6[Mn_2W_{12}O_{43}(H_2O)_8(OH)_8]\cdot 8H_2O$ = 110g

Mass loading of $Na_{12}H_6[Mn_2W_{12}O_{43}(H_2O)_8(OH)_8]\cdot 8H_2O$ on carbon cloth = (2/3) ×5mg = 3.33mg = 3.33×10^{-3}g

Molar mass of Mn = 55 g mole^{-1}

Mass of Mn loading on carbon cloth = {(110×3.33×10^{-3})/3694.08}g = 1×10^{-4}g = (1×10^{-4}g)/(60 g mole^{-1}) = 1.7×10^{-6} mole

Number of Mn atoms present on carbon cloth=1.7×10^{-6}mole=1.7×10^{-6}×6.0221×10^{23}=1.02×10^{18}

Surface concentration (Γ): (1.02×10^{18}/surface area of carbon cloth) = 5.12×10^{17}

TOF value for HER:

$$TOF = \frac{j\,N_A}{Fn\Gamma} = \frac{10 \times 10^{-3} cm^{-2} \times (6.0221 \times 10^{23}\, atoms\, mol^{-1})}{96485\, s\, mol^{-1} \times 2 \times (5.12 \times 10^{17}\, atoms\, cm^{-2})} = 0.061\ s^{-1}$$

TOF value for OER experiment at overpotential of 360 mV (1.59 V vs. RHE):

$$TOF = \frac{j\,N_A}{Fn\Gamma} = \frac{10 \times 10^{-3} cm^{-2} \times (6.0221 \times 10^{23}\,atoms\,mol^{-1})}{96485\,s\,mol^{-1} \times 4 \times (5.12 \times 10^{17}\,atoms\,cm^{-2})} = 0.0305 s^{-1}$$

Table S8 Theoretical and experimental values of decomposed water and FE

H_2 yield(mL)			
Time(s)	Theoretical H_2(mL)	Experimental H_2(mL)	FE (%)
120	7.3	7	96
150	9.15	9	98
180	10.97	11	100
210	12.81	12.5	98
240	14.6	14.5	99
270	16.47	16	97
300	18.2	18	99
330	20.13	20	99
O_2 yield(mL)			
Time(s)	Theoretical O_2(mL)	Experimental O_2(mL)	FE (%)
120	3.6	3.5	97
150	4.5	4.5	100
180	5.5	5.5	100
210	6.4	6.5	100
240	7.3	7	96
270	8.2	8	98
300	9.1	9	99
330	10	10	100

3 REFERENCES

S1 Jun-Sheng Qin, Dong-Ying Du, Wei Guan, Xiang-Jie Bo, Ya-Fei Li, Li-Ping Guo, Zhong-Min Su, Yuan-Yuan Wang, Ya-Qian Lan, Hong-Cai Zhou; Ultrastable Polymolybdate-Based Metal–Organic Frameworks as Highly Active Electrocatalysts for Hydrogen Generation from Water.Journal of the American Chemical Society, 2015, 137, 22: 7169-7177.

S2 Tanmay Rom, Rathindranath Biswas, Krishna Kanta Haldar, Uttam Saha, c Sudhindra Rayaprol, d and Avijit Kumar Paul, Vanadate Encapsulated Polyoxoborate Framework with $[V_{12}B_{18}]$ Cluster: An Efficient Bifunctional Electrocatalyst for Oxygen and Hydrogen Evolution Reactions. Crystal Growth & Design, 2022, 22: 4666-4672.

S3 Jebaslinhepzybai B T, Samaraj E, Kesavan T, et al. Enhanced electrocatalytic activity of in situ carbon encapsulated molybdenum phosphide derived from a hybrid POM for the HER over a wide pH range[J]. Sustainable Energy & Fuels, 2022, 6(2): 289-298.

S4 Tang Y J, Chen Y, Zhu H J, et al. Solid-phase hot-pressing synthesis of POMOFs on carbon cloth and derived phosphides for all pH value hydrogen evolution[J]. Journal of Materials Chemistry A, 2018, 6(44): 21969-21977.

S5 Shekurov, R. et. al. Zn and Co Redox Active Coordination Polymers as Efficient Electrocatalyst, Dalton Trans. 2019, 48: 3601-3609.

S6 Zhou, B.; Zheng, J.; Duan, J.; Hou, C.; Wang, Y.; Jin, W.; Xu, Q. Chemically Robust, Cu-based Porous Coordination Polymer Nanosheets for Efficient Hydrogen Evolution: Experimental and Theoretical Studies. ACS Appl. Mater. Interfaces 2019, 11: 21086-21093.

S7 Chakraborty, D.; Chowdhury, A.; Chandra, M.; Jana, R.; Shyamal, S.; Bhunia, M. K.; Chandra, D.; Hara, M.; Pradhan, D.; Datta, A.; Bhaumik, A. Novel Tetradentate Phosphonate Ligand Based Bioinspired Co Metal−Organic Frameworks: Robust Electrocatalyst for the Hydrogen Evolution Reaction in Different Mediums. Cryst. Growth Des. 2021, 21: 2614-2623.

S8 Wenjing Luo, Jun Hu , Hongling Diao, Benjamin Schwarz, Carsten Streb, and Yu-Fei Song; Robust Polyoxometalate/Nickel Foam Composite Electrodes for Sustained Electrochemical Oxygen Evolution at High pH. Communication,2017,56,18: 4941-4944.

S9 Zhongyuan Yu, Tong Lin, Chunfeng Zhu, Jintang Li, and Xuetao Luo; Design of Trimetallic NiMoFe Hollow Microspheres with Polyoxometalate-Based Metal-Organic Frameworks for Enhanced Oxygen Evolution Reaction. ChemElectroChem, 2021, 8: 1316-1321.

S10 Rom, T.; Biswas, R.; Haldar, K. K.; Sarkar, S.; Saha, U.; Paul, A. K. Charge Separated OneDimensional Hybrid Cobalt/Nickel Phosphonate Frameworks: A Facile Approach to Design Bifunctional Electrocatalyst for Oxygen Evolution and Hydrogen Evolution Reactions. Inorg. Chem. 2021, 60: 15106-15111.

S11 Masa, J.; Weide, P.; Peeters, D.; Sinev, I.; Xia, W.; Sun, Z.; Somsen, C.; Muhler, M.; Schuhmann, W. Amorphous Cobalt Boride (Co_2B) as a Highly Efficient Nonprecious Catalyst for Electrochemical Water Splitting: Oxygen and Hydrogen Evolution. Adv. Energy Mater. 2016, 6: 1502313.

S12 Li, J.; Liu, P.; Mao, J.; Yan, J.; Song, W. Two-Dimensional Conductive Metal-Organic Frameworks with Dual Metal Sites Toward Electrochemical Oxygen Evolution Reaction. J. Mater. Chem. A 2021, 9: 1623-1629.

S13 Wang Y, Wang Y, Zhang L, et al. PBA@POM hybrids as efficient electrocatalysts for the oxygen evolution reaction. Chemistry–An Asian Journal, 2019, 14(16): 2790-2795.

S14 Abdelkader-Fernandez V K, Fernandes D M, Balula S S, et al. Oxygen evolution reaction electrocatalytic improvement in POM@ZIF nanocomposites: a bidirectional synergistic effect. ACS Applied Energy Materials, 2020, 3(3): 2925-2934.
S15 Xing, X.; Liu, R.; Cao, K.; Kaiser, U.; Zhang, G.; Streb, C. Manganese Vanadium Oxide–N-doped Reduced Graphene Oxide Composites as Oxygen Reduction and Oxygen Evolution Electrocatalysts. ACS Appl. Mater. Interfaces 2018, 10: 44511-44517.
S16 Ahmad W, Gao Q, Zhang X L, et al. Sandwich-Type Polyoxometalate Mediates Cobalt Diselenide for Hydrogen Evolution in Acidic Electrolyte. ChemNanoMat, 2020, 6(8): 1164-1168.
S17 Hou Y, Pang H, Zhang L, et al. Highly dispersive bimetallic sulfides afforded by crystalline polyoxometalate-based coordination polymer precursors for efficient hydrogen evolution reaction. Journal of Power Sources, 2020, 446: 227319.
S18 Mitchell G. S. da Silva, Celisnolia M. Leite, Marco A. L. Cordeiro, Valmor R. Mastelaro, and Edson R. Leite; One-Step Synthesis of Nickel Sulfides and Their Electrocatalytic Activities for Hydrogen Evolution Reaction: A Case Study of Crystalline h-NiS and o-Ni_9S_8 Nanoparticles. ACS Applied Energy Materials, 2020, 3, 10: 9498-9503.
S19 Jadranka M, Filipe G, Sara K, Nemanja G, Anup P, Diogo M. F. S and Biljana Š; Transition Metal-Based Polyoxometalates for Oxygen Electrode Bifunctional Electrocatalysis. Batteries, 2024, 10(6), 197.
S20 Yajie L, Na Z, Zhixuan S, Xiaoli H, Zhiyu D and Zhongmin S; An hourglass-shaped nickel-based polyoxometalate crystalline material as a highly efficient bifunctional electrocatalyst for the oxygen evolution reaction and detection of H_2O_2.Inorganic Chemistry Frontiers,2024,11, 2598-2607.
S21 Xin-Bao H, Dong-Xue W, Eduardo G, Yu-Hui Luo d, Yuan-Zhi T, Dong-Fei L, Yang-Guang L, Thomas W, En-Bo W, Lan-Sun Z; Fe-substituted cobalt-phosphate polyoxometalates as enhanced oxygen evolution catalysts in acidic media. Chinese Journal of Catalysis, 2020,41,5,853-857.
S22 Ali H I, Reza O, Jahan-Bakhsh R; Novel polyoxometalate-based composite as efficient electrocatalyst for alkaline water oxidation reaction. Journal of the Iranian Chemical Society, 2021,18,2079-2089.
S23 Huang Y, Ma Z, Hu Y, Chai D, Qiu Y, Gao G, Hu P; An efficient $WSe_2/Co_{0.85}Se$/graphene hybrid catalyst for electrochemical hydrogen evolution reaction. RSC Advances,2016, 6 (57), 51725−51731.
S24 Nimai B, Pravin P. I, Suddhasatwa B; Electrosynthesis of Mn-Fe oxide nanopetals on carbon paper as bi-functional electrocatalyst for oxygen reduction and oxygen evolution reaction. International Journal of Hydrogen Energy,2018,43,6,3165-3171.
S25 Conghui S., Yelong Z., Changqin Z., Hui G., Wensheng M., Lanfen L., Zhonghua Z.; Mesoporous nanostructured spinel-type MFe_2O_4(M = Co, Mn, Ni) oxides as efficient bi-functional electrocatalysts towards oxygen reduction and oxygen evolution. Electrochimica Acta,2017, 245, 829-838.
S26 Carsten W, Dr. P W. M, Dr. S L, Prof. Dr. H D, Prof. Dr. M D; Facile Formation of Nanostructured Manganese Oxide Films as High-Performance Catalysts for the Oxygen Evolution Reaction. ChemSusChem,2018,11,15,2554-2561.
S27 Hongtao C., Lige G., Jihua W., Limin D., Jingyu Z., Yitong M., Binghe Y., Meijia W., Yunhao G., Hui L.; POM@TM-MOFs prism-structures as a superior bifunctional electrocatalyst for overall water splitting. Journal of Solid State Chemistry,2024,331,124550.
S28 Linghao H., Shunjiang H., Yongkang L., Minghua W., Bingbing C., Shide W., Jiameng L., Zhihong Z., Miao D.; Multicomponent Co_9S_8@MoS_2 nanohybrids as a novel trifunctional electrocatalyst for efficient methanol electrooxidation and overall water splitting. Journal of Colloid and Interface Science, 2021, 586, 538-550.

S29 Jagadis G., Yi L., Jie G., Zhiyuan M., Bipeen D., Aadil Nabi C., Lubin N., Guowang D., Yongge W.; Three-Dimensional Nano Assembly of Nickel Cobalt Sulphide/Polyaniline@Polyoxometalate/Reduced Graphene Oxide Hybrid with Superior Lithium Storage and Electrocatalytic Properties for Hydrogen Evolution Reaction**.** Journal of Colloid and Interface Science, 2022, 614, 642-654.

S30 Cheolmin L., Dasom J., Jehee P., Wonsuk L., Jaehyun P., Seok Ju K., Youngsik K., Jungki R.; Tetraruthenium Polyoxometalate as an Atom-Efficient Bifunctional Oxygen Evolution Reaction/Oxygen Reduction Reaction Catalyst and Its Application in Seawater Batteries. ACS Applied Materials & Interface*s*, 2020, 12(29), 32689-32697.

S31 Yukun L., Changle Y., Yaping L., Wenjing B., Xinxin G., Wenfeng Y., Zhi L., Ping J., Wenfu Y., Shoujie L., Yuan P., Yunqi L.; Atomically dispersed Ni on Mo_2C embedded in N, P co-doped carbon derived from polyoxometalate supramolecule for high-efficiency hydrogen evolution electrocatalysis. Applied Catalysis B: Environment and Energy, 2021,296,5, 120336.

S32 Jing J., Qiuxia L., Chunmei Z., Lunhong A.; Cobalt/molybdenum carbide@ N-doped carbon as a bifunctional electrocatalyst for hydrogen and oxygen evolution reactions. Journal of Materials Chemistry A,2017,5, 16929-16935.

S33 Xiaobin X., Farhat N., Xun W.; Ni-decorated molybdenum carbide hollow structure derived from carbon-coated metal-organic framework for electrocatalytic hydrogen evolution reaction.Chemistry of Materials, 2016, 28, 17, 6313-6320.

S34 Jiao D., Wentao Y., Pengju R., Yong W., Dehui D., Ze Zh., Xinhe B.; High performance hydrogen evolution electrocatalysis by layer-controlled MoS_2 nanosheets.RSC Advances, 2014,4, 34733-34738.

S35 Zheng H., Zhuxian Y., Quanli J., Nannan W., Yanqiu Z., Yongde X.;Bimetallic Co-Mo sulfide/carbon composites derived from polyoxometalate encapsulated polydopamine-decorated ZIF nanocubes for efficient hydrogen and oxygen evolution.Nanoscale, 2022,14, 4726-4739.

S36 Ganga S., Subhasis D A., Debaprasad M.; Stabilization and Activation of Polyoxometalate over Poly(Vinyl Butylimidazolium) Cations towards Electrocatalytic Water Oxidation in Alkaline Media. Chemical Communications,2023, 59, 4774-4777.

S37 Yupeng Z., Dandan G., Johannes B., Ute K., Rongji L., Carsten S.; Polyoxometalate-Assisted Synthesis of Amorphous Zeolitic Imidazolate for Efffcient Electrocatalytic Oxygen Evolution. Results in Chemistry,2022, 4, 100568.